RESTRICTED

COPY NO. 8
RM No. E7G30

Unclass. by auth. H. L. Dryden per NACA Release form #1241 - 6/5/53

23 OCT 1947

RESEARCH MEMORANDUM

COOLING OF GAS TURBINES

VII - EFFECTIVENESS OF AIR COOLING OF HOLLOW

TURBINE BLADES WITH INSERTS

By Joseph R. Bressman and John N. B. Livingood

Flight Propulsion Research Laboratory
Cleveland, Ohio

CLASSIFIED DOCUMENT

TECHNICAL EDITING WAIVED

NATIONAL ADVISORY COMMITTEE FOR AERONAUTICS

WASHINGTON

October 20, 1947

RESTRICTED

NATIONAL ADVISORY COMMITTEE FOR AERONAUTICS

RESEARCH MEMORANDUM

COOLING OF GAS TURBINES

VII - EFFECTIVENESS OF AIR COOLING OF HOLLOW TURBINE BLADES WITH INSERTS

By Joseph R. Bressman and John N. B. Livingood

SUMMARY

An analytical investigation was made to determine primarily the reduction in cooling-air requirement and the increase in effective gas temperature for the same quantity of cooling air resulting from the use of an insert in the cooling-air passage of a hollow air-cooled turbine blade. The insert provided an annular cooling-air passage and lowered the ratio of cooling-air-flow area to minimum hot-gas-flow area per blade. Equations for the blade radial stress and temperature distribution were derived and the analysis was applied to a specific turbine using three blade designs: a hollow blade and two blades with different inserts. A secondary object of the investigation was to obtain the effect on dilution of neglecting radiation from the nozzles to the turbine blade, radiation from the inner blade wall to the insert, and radial heat conduction, both separately and collectively, for a hollow-blade design with an insert and for fixed values of the effective gas temperature, average insert temperature, and turbine tip speed. The effects on blade temperature of variations in blade-root temperature, average insert temperature, and blade-root cooling-air temperature were also investigated for a specific effective gas temperature and dilution.

For a hollow air-cooled turbine blade with an insert, which reduced the ratio of cooling-air-flow area to minimum hot-gas-flow area per blade approximately one-half, and for a limiting cooling-air Mach number of 0.50 at the blade root, the air mass flow for adequate cooling of the blade was reduced two-thirds and three-fifths below that for a blade with no insert for effective gas temperatures of 1900° and 1700° F, respectively. The blade Mach numbers were found to be 0.55 and 0.53 for effective gas temperatures of 1900° and 1700° F, respectively. For the same blade-insert design and a dilution of 3 percent, the effective gas temperature was increased 310° F above that for a blade with no insert at a blade Mach number of 0.50. For the same blade-insert design and typical turbine

operating conditions, it was found that neglecting radiation from the nozzles to the blade, radiation from the inner blade wall to the insert, or radial heat conduction decreased the dilution about 0.25 percent, increased the dilution about 0.25 percent, and increased the dilution about 0.10 percent, respectively, for safe operation at the critical blade point. Neglecting all three sources of heat transfer collectively resulted in so slight a change in dilution that a 3-percent dilution was shown to be sufficient for safe operation at the design tip speed of 1300 feet per second. In general, the temperature-distribution curves were shown to be nearly the same from the blade tip to a point near the blade root; at the blade root, the curve including radiation and radial heat-conduction effects rapidly diverged from the curve excluding these effects. For this same blade-insert design, it was found that a 100° F change in blade-root temperature, average insert temperature, or blade-root cooling-air temperature resulted in a change in the temperature of the critical section of the blade of 7.5° F, 27° F, and 30° F, respectively.

INTRODUCTION

The problem of utilizing high temperatures in gas turbines and jet-propulsion engines has been approached from two directions: the development of high-strength, high-temperature materials and the cooling of the materials currently in use. High-temperature materials currently available limit temperatures at the turbine inlet to approximately 1500° F; consequently, in order to utilize higher temperatures, it is necessary to resort to cooling. Turbine-blade cooling has several disadvantages: (1) The mechanical complexity of the engine increases; (2) a power loss occurs in circulating the cooling medium, although with schemes for regenerative cooling a heat loss or a loss in working fluid is not inevitable; (3) the manufacturing problems appear to limit blade forms when compared with solid blades; and (4) many blade-dimension parameters chosen for good cooling may not be satisfactory when aerodynamic blade performance is considered. In order to warrant the use of cooling, the heat-transfer process must be an efficient one.

Research recently reported in this country and abroad on the cooling of turbine blades (references 1 to 12) considers methods of indirect cooling by conducting heat away from the blade and direct cooling by air or liquids flowing in hollow passages in the blade. The analyses demonstrated that, for high-power turbines with long blades and high specific mass flows, increases in gas temperatures of the order of 100° to 200° F were possible with indirect cooling. Considerably greater increases in gas temperature were made possible by direct cooling with either water or air as the coolant. Although the potential increases in gas temperature are not as great with air cooling as with liquid cooling, air cooling involves less mechanical complication and avoids the necessity of a cooling medium with its attendant ducting and heat exchangers. Of the air-cooling methods discussed in the foregoing references, the method of boundary-layer cooling (references 9 and 11) requires the smallest quantity of cooling air, but a considerable stress and manufacturing problem is associated with this scheme.

Reference 7 presents a general method of analysis for temperature and stress distribution in a hollow air-cooled turbine blade but neglects the effects of radiation and conduction. A study of reference 7 suggests that the cooling-air requirement could be decreased considerably if the cooling air is forced to flow through an annular passage formed by the inner wall of the blade and an insert placed in the hollow blade. Blades of this type have already been manufactured in mass production for a German jet engine.

An analysis is developed herein for the temperature and the stress distribution of a hollow air-cooled turbine blade with an insert; effects of radiation, conduction, and cooling-air temperature rise due to compression occurring in the passage through the turbine blades are included. The primary purpose of this analysis is to show the reduction in cooling-air requirement for given operating conditions and the increase in effective gas temperature for the same quantity of cooling air resulting from the use of an insert in the blade cooling-air passage. Effects of radiation from the nozzles to the turbine blades, radiation from the inner blade wall to the insert, and radial heat conduction on dilution are also given for selected operating conditions. In addition, the effects on blade temperature of variations in blade-root temperature, average insert temperature, and blade-root cooling-air temperature are given; calculations are also included to determine the heat loss to the cooling air.

A conventional gas-turbine-blade design was chosen for the application of the analysis. The cooled turbine was assumed to be operating at the design conditions of turbine-inlet pressure, rotational speed, and mass flow. The hollow blade was designed for the same tip-to-root ratio for metal cross-sectional area as the uncooled blade. Three ratios of cooling-air-flow area to minimum hot-gas-flow area per blade were investigated. The radial stress distribution and the permissible blade temperatures (based on stress-rupture data for cast S-816 high-temperature alloy) were calculated.

ANALYSIS OF TURBINE-BLADE TEMPERATURE AND STRESS DISTRIBUTION

Assumptions

In deriving the equations for temperature and stress distribution, the following assumptions were made:

1. The hollow blades have a constant external cross-sectional area and perimeter over the blade height.

2. For the purposes of stress calculation, the blade wall varies in thickness from the root to the tip.

3. For the purposes of heat-transfer calculation, the dimension of the blade-root section (area, perimeter, and thickness) exist over the blade height.

4. Heat is conducted in a radial direction only; the heat flows through the blade wall with a negligible temperature differential.

5. The blade temperature is constant over any cross section.

6. The Prandtl number of the cooling air remains constant throughout the blade.

7. The outside heat-transfer coefficient is constant over the blade outer surface.

8. The effective gas temperature is constant over the blade outer surface.

9. The inside heat-transfer coefficient is constant over the inner surface of the blade.

10. The only surfaces radiating heat to the blades are the turbine nozzles.

11. No external surfaces are colder than the rotor blades to which the rotor blades could radiate heat.

12. The turbine nozzles are at the effective gas temperature relative to the rotor blades.

13. The emissivity factors for the nozzle, blade, and insert surfaces remain constant at mean values over the blade height.

14. The radiation coefficients for nozzle, blade, and insert surfaces remain constant at mean values over the blade height.

15. The insert temperature remains constant at a mean value over the blade height.

16. Bending stresses or stress concentrations are ignored. The stress is constant over any blade cross section and is equal to the calculated centrifugal stress at that cross section.

17. The insert is self-supporting and does not increase the stress in the blade.

18. The criterion of blade failure is the stress-rupture properties of the blade material.

Validity of Assumptions

In assumption 3, the dimensions of the root section rather than average dimensions for the blade height are assumed because the critical section of the blade, the point where failure will first occur, is 10 to 15 percent of the height from the root.

Assumption 4 is satisfactory in the thin portions of the blade near the tip. Near the root where the blade wall is thick, however, the neglect of transverse conduction has some effect on blade temperatures (for typical operating conditions, the outside blade-wall temperature was found to be 22° F greater than the average temperature used), but has little effect on dilution requirements or allowable gas-temperature increase for a given dilution.

If no heat were removed from the turbine nozzles, they would assume a temperature close to the turbine-inlet total temperature; however, heat is radiated to the cooler turbine rotor blades and conducted to the cooler casing and inner shroud. As a result, it is assumed (assumption 12) that the nozzle temperature is reduced to the effective gas temperature relative to the blades. (See reference 10, p. 72.)

The assumption of a constant mean value for the insert temperature (assumption 15) results in a calculated value of blade-metal temperature at the root, which is higher than the blade-metal temperature that would exist with a variation in insert temperature from root to tip. Inasmuch as the linearized radiation coefficient from the blade wall to the insert is considerably smaller than the cooling-air heat-transfer coefficient, the insert temperature at any position would differ only slightly from the cooling-air temperature at that position. At the critical section, the cooling-air temperature and, consequently, the insert temperature is low and if the assumed value of insert temperature is greater than the actual value, the calculated value of heat radiated from the blade to the insert would be lower than the actual value. The calculated blade temperature at the critical section would therefore be higher than the actual temperature. At the tip, the reverse conditions exist and the calculated temperature would be lower than the actual temperature.

Temperature Distribution

The symbols used in the analysis are defined in appendix A. The equation for the radial temperature distribution in the blade is derived in detail in appendix B. A heat balance for a small section of the blade results in the following differential equation for the average blade-metal temperature:

$$\frac{d^3t_m}{dy^3} + Y\frac{d^2t_m}{dy^2} - (\alpha + \beta + \delta)\frac{dt_m}{dy} + \left[\frac{h_i p_i}{m_a c_p}\delta - Y(\alpha + \beta + \delta)\right]t_m$$

$$= -\frac{\omega^2\delta}{gc_pJ}y - \left[\frac{\omega^2\delta}{gc_pJ}r_r + \left(\frac{h_i p_p}{m_a c_p}\delta + Y\beta\right)t_p + Y\alpha t_e\right] \qquad (1)$$

Inasmuch as little data are available on the value of the heat-transfer coefficient for the outside surface of a turbine blade, the following equation used in reference 7 was assumed to hold true:

$$h_o = 0.0323\ G_g^{0.685}\ p_o^{-0.315}$$

Reference 13 (p. 170, equation (4f)) suggests the following equation for the heat-transfer coefficient in annular spaces, which was used to calculate the heat-transfer coefficient inside the blade;

$$h_i = 0.020\left(\frac{D_l G_a}{\mu_a}\right)^{0.8}\frac{k_a}{D_l}$$

where

$$D_l = \frac{4A_l}{p_i + p_p}$$

and

$$A_l = A_i - A_p$$

(reference 13, pp. 200 and 202, equation (24)). The diameter D_l is the hydraulic diameter for the cooling-air passage and μ_a and k_a are determined for a temperature of 400° F. For the blade without an insert, $p_p = 0$ and $D_l = 4A_l/p_i$. If the change in h_i due to the variation in the ratio $k_a/\mu_a^{0.8}$ with temperature is neglected, the heat-transfer coefficient inside the blade remains constant along the blade height.

The coefficients h_n and h_p are calculated as the product of the radiation interchange factor E and h_r the radiation coefficient. The interchange factor E is a function of the emissivity of the radiating surface, the absorption of the receiving surface, the surface areas of the radiating and absorbing surfaces, and a factor $\overline{F}$ given in terms of direct geometrical factors.

For any particular set of operating conditions, the coefficients in equation (1) are constants that can be numerically evaluated and the equation becomes a linear differential equation with constant coefficients. A general solution of the equation is given in the following form:

$$t_m = c_1 e^{\lambda_1 y} + c_2 e^{\lambda_2 y} + c_3 e^{\lambda_3 y} + c_4 y + c_5 \tag{2}$$

The evaluation of the five constants in equation (2) is given in appendix B.

Stress Distribution

The equation for the centrifugal stress at any cross section y in a linearly tapered blade, as derived in appendix C, is:

$$s = \frac{\rho_m v^2}{2g\left[\left(\frac{A_{m,t}}{A_{m,r}} - 1\right)\frac{y}{L} + 1\right]}\left\{\left(\frac{A_{m,t}}{A_{m,r}} - 1\right)\left[\frac{r_t}{L} - 1 + \frac{2}{3}\frac{y}{L}\right]\left(\frac{y}{r_t}\right)^2 + \left[2\left(1 - \frac{L}{r_t}\right)\frac{y}{r_t} + \left(\frac{y}{r_t}\right)^2\right]\right\}_y^L \tag{3}$$

The equations for temperature and stress distribution were used for the following reasons: (1) to determine the reduction in cooling-air mass-flow requirement resulting from the use of an insert placed in the cooling-air passage; (2) to calculate the effect of neglecting radiation from the nozzles, radiation to the insert, and radial heat conduction on dilution; (3) to calculate the effect on blade temperature of changes in factors such as blade-root temperature, average insert temperature, and blade-root cooling-air temperature; (4) to determine the effect of neglecting transverse conduction through the wall; and (5) to calculate the heat loss to the cooling air.

APPLICATIONS OF ANALYSIS

Effect of Insert on Cooling-Air Requirements and Effective Gas-Temperature Increase

The temperature and stress distributions were calculated for three air-cooled turbine blades: one blade without an insert (fig. 1(a)) and two blades with inserts of different size placed inside the cooling-air passage (figs. 1(b) and 1(c)). The external blade shape was chosen from the rotor root section of a conventional gas-turbine design. The blade wall varies from a thickness of 0.060 inch at the root to 0.020 inch at the tip, which gives a tip-to-root ratio of 0.333 for the blade-metal cross-sectional area. The turbine-blade dimensions are given in table I.

The blade temperatures at various positions were calculated from equation (2) and plotted as a function of the blade position. The stress at various blade positions was computed for various tip speeds by means of equation (3) and the permissible temperature corresponding to the stress at any blade position was taken from stress-to-rupture data (fig. 2). These calculations gave the permissible radial-temperature distribution, which was plotted with the calculated temperature distributions. The curve of permissible blade-temperature distribution shows the maximum safe operating temperature permitted at any point on the blade for a particular blade tip speed. If the curve of calculated blade-temperature distribution crosses that of the permissible blade-temperature distribution, the blade will be too hot for design life in the region between the two curves and will presumably fail by rupture earlier than anticipated. In order for the blade to operate safely as designed, the curve of calculated temperature distribution should be below the curve of permissible temperature distribution or, at least tangent to the curve of permissible temperature distribution at the critical section and below it at all other points. (See figs. 3 to 5.)

Effective gas temperatures of 1700° and 1900° F corresponding to turbine-inlet total temperatures of 1920° and 2140° F, respectively, were considered. The relation between the absolute effective gas temperature and the absolute turbine-inlet temperature is derived in appendix D. For an ideal impulse turbine operating at the optimum blade-jet speed ratio, the ratio of absolute effective gas temperature to absolute turbine-inlet temperature is 0.907. The temperature distributions in the blades were calculated for various dilutions (ratio of cooling-air mass flow to hot-gas mass flow) for each blade. The dilutions were so chosen that the cooling-air Mach number at the root M_a was less than 0.50 and it was assumed that the cooling-air temperature at the root was 400° F. A blade-metal temperature at the root was assumed and equation (1) solved. If the assumed root temperature was less than 150° F below the calculated temperature at the critical section, a new root temperature was assumed and equation (1) was re-solved. The root temperature was chosen as 150° F below the critical temperature because it has been found (reference 3) that larger temperature differentials do not appreciably affect the blade temperatures near the critical portion of the blade.

In order to determine the radiation coefficient and the interchange factor E, it was necessary to assume values of emissivity for the radiating and absorbing surfaces. The values of emissivity were chosen from the factors given for nickel alloys in reference 13. The emissivity of the blade surface was assumed to be 0.90 for an average blade temperature of 1400° F and that for the nozzle surface was assumed to be 0.95 for nozzle temperatures of 1700° and 1900° F, which are the same as the corresponding effective gas temperatures. The values for the factors $\bar{F}_{n,m}$ and $\bar{F}_{m,p}$ were taken as unity because the surfaces considered are nearly the same as surfaces for which these factors have been found to equal unity. The use of these assumed factors resulted in values of nozzle radiation coefficients $h_n = E_{n,m}\, h_r$ of 56 for a nozzle temperature of 1900° F and 43 for a nozzle temperature of 1700° F. These nozzle radiation coefficients were assumed to remain constant for all variations in average blade temperature. The emissivity of the insert surface was chosen as 0.5 for an average temperature of 600° F for blade 2 and 700° F for blade 3. This value of emissivity and the assumed value of unity for $\bar{F}_{m,p}$ resulted in an average value of the radiation coefficient from the inside blade wall to the insert surface $h_p = E_{m,p}\, h_r$ of 12. Additional turbine operating factors are listed in table II.

The blade metal chosen was cast S-816. The stress-to-rupture strength for 1000 hours as a function of temperature for this alloy is plotted in figure 2. (See reference 14.) The stresses and corresponding permissible temperatures were calculated for the design tip speed of 1300 feet per second and for speeds of 1200 and 1400 feet per second in order to show the required change in tip speed for safe operation.

Calculations were also made in order to plot the increase in effective gas temperature against dilution for blades 1 and 3 at a blade Mach number M (ratio of tip speed to sonic velocity of hot gas at the effective gas temperature) of 0.50. Blade 2 was not considered in this investigation; the calculations were intended only to compare the blade without an insert to the blade with an insert. Lines of constant cooling-air Mach number M_a (ratio of velocity of cooling air within the blade to the critical velocity of the cooling air) were superimposed. The critical velocity of the cooling air ($M_a = 1.0$) is $\sqrt{\frac{2}{\gamma + 1} \gamma g R (T_a + 460)}$.

Effect of Neglecting Radiation and Radial Heat Conduction on Dilution

For a constant design tip speed of 1300 feet per second, an effective gas temperature of 1900° F, and an average insert temperature of 700° F, temperature distributions were obtained for blade 3 for various dilutions with nozzle radiation, insert radiation, and radial heat conduction neglected separately and collectively. The distributions, with nozzle and insert radiation neglected, were obtained by solving equation (1) with $h_n = 0$ and $h_p = 0$ and by applying the following boundary conditions:

$$t_{m,r} = 1200^\circ \text{ F, when } y = 0$$

$$t_{a,r} = 400^\circ \text{ F, when } y = 0$$

$$\frac{dt_m}{dy} = 0, \text{ when } y = L$$

These boundary conditions are the same as those used when the effect of radiation was included.

When radial heat conduction was neglected, the order of the differential equation expressing the temperature distribution through the turbine blade was reduced from 3 to 1. The equation was derived (appendix B) with $Q_1 = Q_2 = 0$; the heat balance was found to be

$$(h_n b + h_o p_o)(t_e - t_m) = h_i p_i(t_m - t_a) + h_p p_i(t_m - t_p)$$

Substitution for t_a and simplification reduces this equation to

$$\frac{dt_m}{dy} + \left(Y - \frac{h_i p_i}{m_a c_p} Z\right) t_m = \frac{\omega^2}{g c_p J} Z \cdot y$$

$$+ Z\left[\frac{\omega^2 r_r}{g c_p J} + \frac{(h_n b + h_o p_o)}{h_i p_i} Y t_e + \left(\frac{h_p}{h_i} Y + \frac{h_i p_p}{m_a c_p}\right) t_p\right] \qquad (4)$$

where

$$Z = \frac{h_i p_i}{(h_n b + h_o p_o + h_i p_i + h_p p_i)}$$

For any set of turbine operating conditions, the coefficients become constants and the equation is easily solved, being linear and of the first order. The boundary condition chosen was $t_{a,r} = 400^\circ$ F, when $y = 0$ to correspond to one previously used in order to compare results. Without conduction, moreover, a rim temperature of 1200° F was no longer justified; with $t_{a,r} = 400^\circ$ F, the rim temperature was found to be about 1335° F.

The effect of neglecting nozzle radiation, insert radiation, and radial conduction collectively was found by solving equation (4) with $h_n = h_p = 0$, and by using the same boundary condition $t_{a,r} = 400^\circ$ F, when $y = 0$.

Effect of Changes in Analysis Factors on Blade Temperature

In order to demonstrate the relative importance of various factors in the analysis, the effect of a variation in these factors on the blade-temperature distribution for blade 3 was determined. Blade-root temperatures of 1100°, 1200°, and 1300° F, average insert temperatures of 600°, 700°, and 800° F, and blade-root cooling-air temperatures of 300°, 400°, and 500° F were considered. The calculations were made for a dilution of 3 percent and an effective gas temperature of 1900° F. Other turbine operating conditions for blade 3 were the same as in the calculations for the effect of the insert.

Heat Loss to Cooling Air

In order to calculate the heat loss to the cooling air, it is necessary to determine the cooling-air temperature rise. The cooling-air temperature distribution was calculated by means of equation (12) in appendix B for blade 3 with 3-percent dilution and for blade 1 with 10-percent dilution for an effective gas temperature of 1900° F. Other turbine operating conditions for these calculations were the same as in the preceding calculations. From a determination of the temperature rise of the cooling air, the cooling-air mass flow, and a mean value of specific heat, the amount of heat absorbed by the cooling medium can be calculated. The enthalpy drop through the turbine can be found by the following equation if the total-pressure ratio across the turbine is assumed equal to the critical pressure ratio across the nozzles (absolute exit velocity neglected):

$$\frac{\text{Actual enthalpy drop}}{\text{Blade}} = \frac{m_g c_p (T_g + 460)}{\eta_t}\left[1 - \left(\frac{P_{n,2}}{P_{n,1}}\right)^{\frac{\gamma - 1}{\gamma}}\right] \tag{5}$$

where

$$\eta_t = 85 \text{ percent}$$

$$T_g = 2180^\circ \text{ F}$$

$$\left(\frac{P_{n,2}}{P_{n,1}}\right) = \left(\frac{2}{\gamma + 1}\right)^{\frac{\gamma}{\gamma - 1}} = 0.544 \text{ for } \gamma = 1.317$$

The heat loss to the cooling fluid can then be found as a percentage of the turbine enthalpy drop.

RESULTS AND DISCUSSION

Effect of Insert

The results of the calculations for blades 1, 2, and 3 are shown in figures 3, 4, and 5, respectively. For an effective gas temperature t_e of 1900° F and a limiting cooling-air Mach number of 0.50, it would require slightly more than 10-percent dilution for blade 1, slightly more than 5-percent dilution for blade 2, and 3-percent dilution for blade 3 to cool the critical section of the blade (10 to 15 percent of height from the root) below the permissible temperature corresponding to the design tip speed of 1300 feet per second. At an effective gas temperature of 1700° F, slightly more than 5-percent dilution for blade 1, 3-percent dilution for blade 2, and about 2-percent dilution for blade 3 is necessary to cool the critical section below the permissible temperature.

A comparison of the results for blade 1 with those for blade 3 indicates that a safe operating point for blade 3 can be achieved for an effective gas temperature of 1900° F with 3-percent dilution as compared with over 10 percent for blade 1, which is a reduction of over two-thirds the cooling-air requirement. For an effective gas temperature of 1700° F, the reduction is from over 5 percent to 2 percent, a reduction of about three-fifths of the cooling-air requirement.

The effect of the ratio of cooling-air-flow area to minimum hot-gas-flow area on the approximate dilution required for safe operation is shown in figure 6. As the ratio A_l/A_b is reduced, the slope of the curve decreases, which means that the dilution will be slowly reduced with values of A_l/A_b less than 0.4. In other words diminishing returns result from reductions of the ratio A_l/A_b less than roughly 0.4. A low value of this ratio can be achieved by reducing the value of A_l or by lowering the solidity of the turbine (increasing blade spacing) to increase the value of A_b.

Figure 7 shows the increase in effective gas temperature plotted against dilution with lines of constant cooling-air Mach number superimposed for blades 1 and 3; the calculations were made for a blade life of 1000 hours and a blade Mach number of 0.50. For a dilution of 3 percent, the effective gas temperature was increased 310° F by the insert.

Effect of Neglecting Radiation and Radial-Heat Conduction on Dilution

Effect of radiation from nozzles to blade wall. - The effect on dilution of neglecting radiation from the nozzles to the blade wall in blade 3 is shown in figure 8; temperature distributions are given for three dilutions. The results indicate that a dilution of 2.75 percent will suffice for safe operation at the design tip speed of 1300 feet per second; therefore, neglecting nozzle radiation decreased the dilution about 0.25 percent (from 3.00 percent to 2.75 percent). This reduction is smaller than might be expected because the effective blade area for absorbing radiation was only about one-third that of the blade-surface area used in conjunction with the outside heat-transfer equation.

Effect of radiation from inner blade wall to insert. - The effect of neglecting radiation to the insert in blade 3 is shown in figure 9. Temperature distributions were obtained for two dilutions. It was found that neglecting the insert radiation increased the dilution about 0.25 percent (from 3 to 3.25 percent) and still insured safe operation at the design tip speed of 1300 feet per second.

Effect of radial heat conduction. - The effect of neglecting radial heat conduction in blade 3 is shown in figure 10. In this case, the dilution must be increased about 0.10 percent (from 3 to about 3.10 percent) in order to reduce the temperature-distribution curve below the permissible-temperature curve for a design tip speed of 1300 feet per second.

Effect of neglecting radiation from nozzles, radiation to insert, and radial heat conduction. - The effect of collectively neglecting all three sources of heat transfer (fig. 11) is very slight. The 3-percent dilution is sufficient for the design tip speed of 1300 feet per second, which indicates that a good approximation may be obtained by neglecting radiation from the nozzles and to the insert and radial heat conduction, and therefore, by the solution of a simple linear differential equation of the first order. In designing an adequate turbine blade with an insert, this simplified method will suffice for the basic selection of the blade design; the effects of radiation and radial heat conduction can then be included as a refinement.

Effect of Changes in Analysis Factors on Blade-Temperature Distribution

Effect of blade-root temperature. - The effect of blade-root temperatures of 1100°, 1200°, and 1300° F on the temperature distribution in blade 3 is shown in figure 12. These root temperatures correspond to differences between root and critical-section temperatures of approximately 50°, 150°, and 250° F, respectively. The effect of root temperature (or conduction to the root) is small; a 100° F change in root temperature resulted in a 7.5° F maximum change in blade temperature at the critical section and a negligible change over most of the blade height.

Effect of average insert temperature. - The effect of average insert temperatures of 600°, 700°, and 800° F on the temperature distribution in blade 3 is shown in figure 13. A 100° F change in average insert temperature resulted in a 27° F change in the temperature of the critical section. If the insert temperature at the root is the same as the cooling-air temperature at the root and the insert temperature varies linearly with the blade position, a 100° F change in average insert temperature would require a 200° F change in insert temperature at the tip. For a particular set of operating conditions, the insert-temperature distribution is uniquely determined. The assumption of an average insert temperature in the heat-transfer calculation means that the heat removed from the critical section will be less than if the actual insert temperature at the critical section had been used; therefore, the blade-metal temperature t_m at the critical section actually would be somewhat lower than calculated.

Effect of blade-root cooling-air temperature. - The effect of blade-root cooling-air temperatures of 300°, 400°, and 500° F in blade 3 is indicated in figure 14. A 100° F change in blade-root cooling-air temperature resulted in a change at the critical section of approximately 30° F; the change diminishes somewhat toward the tip of the blade. The blade-root cooling-air temperature should therefore be maintained as low as possible.

Loss of Heat to Cooling Air

The cooling-air temperature distributions for blade 1 with 10-percent dilution and for blade 3 with 3-percent dilution are shown in figure 15. The variation in cooling-air temperature was calculated from equation (12) in appendix B. The slope of the curve, or the rate of increase in cooling-air temperature with height for blade 3, is greatest near the root and diminishes gradually toward the tip, which means that the cooling air picks up more heat at the root section than at the tip. This fact is due to the larger temperature differential between the hot gases and cooling air at the root than at the tip.

For an average value c_p of 0.250 and a cooling-air temperature range from 400° to 825° F, the quantity of heat absorbed by the cooling air was calculated as follows:

The temperature of the cooling air increased from 400° to 825° F, or 425° F. If no heat had been transferred to the air, the temperature would have risen 72° F on being compressed isentropically in the blade; consequently, the net temperature rise due to heat absorbed by the cooling air is 353° F and the heat absorbed is 13,900 Btu per hour per blade. The heat absorbed by the cooling air in blade 1 is approximately the same as in blade 3. The enthalpy drop through the turbine calculated by equation (5) for a mean value of c_p for the hot gases of 0.286 was found to be 635,000 Btu per hour per blade. The heat removed from the gas is therefore about 2.2 percent of the enthalpy drop through the turbine. If more energy were taken out of the turbine with a larger pressure drop, the heat removed by the cooling air would be a smaller percentage of the enthalpy drop through the turbine.

SUMMARY OF RESULTS

Results were obtained from an analytical investigation of the effectiveness of air cooling of hollow turbine blades with inserts. For a particular hollow air-cooled turbine blade and set of turbine operating conditions, the use of an insert in the blade, which provided an annular cooling-air passage and reduced the ratio of cooling-air-flow area to minimum hot-gas-flow area per blade from 0.990 to 0.447 gave the following results:

1. For a limiting cooling-air Mach number of 0.50, the required cooling-air mass flow was reduced two-thirds and three-fifths for effective gas temperatures of 1900° and 1700° F, respectively, when the blade with the insert was used in place of the hollow blade; the blade Mach numbers were 0.55 and 0.53 for effective gas temperature of 1900° and 1700° F, respectively.

2. For a dilution of 3 percent, the effective gas temperature was increased 310° F when the blade with the insert was used in place of the hollow blade.

3. For the same blade-insert design, a design tip speed of 1300 feet per second, an effective gas temperature of 1900° F, and an average insert temperature of 700° F, the following results were obtained:

(a) Neglecting radiation from the nozzles to the blade wall decreased the dilution about 0.25 percent.

(b) Neglecting radiation from the inner blade wall to the insert increased the dilution about 0.25 percent.

(c) Neglecting radial heat conduction increased the dilution about 0.10 percent.

(d) Neglecting nozzle radiation, insert radiation, and radial heat conduction collectively had no appreciable effect on the dilution.

(e) Neglecting radiation and radial heat conduction, which simplifies the temperature-distribution equation, gave a good approximation for blade temperatures.

4. For the same blade-insert design, an effective gas temperature of 1900° F, and a dilution of 3 percent, the following results were obtained:

(a) A 100° F change in blade-root temperature resulted in a 7.5° F maximum change in the temperature of the critical section of the blade.

(b) A 100° F change in average insert temperature resulted in a 27° F change in the temperature of the critical section of the blade.

(c) A 100° F change in the blade-root cooling-air temperature resulted in a 30° F change in the temperature of the critical section of the blade.

Flight Propulsion Research Laboratory,
National Advisory Committee for Aeronautics,
Cleveland, Ohio.

APPENDIX A

SYMBOLS

The following symbols are used in this analysis:

A cross-sectional area, sq ft

a_g sonic velocity of hot gases at effective gas temperature, ft/sec

B number of blades

b effective blade width for radiation, $2\pi(r_t - l/2)/B$, ft

c constant

c_p specific heat at constant pressure, Btu/(lb)(°F)

D_l hydraulic diameter of cooling-air passage, $4A_l/(p_i + p_p)$, ft

E radiation interchange factor:

$$E_{n,m} \text{ (nozzles to blades) } = \frac{1}{\frac{1}{\overline{\overline{F}}_{n,m}} + \left(\frac{1}{\epsilon_n} - 1\right) + \frac{S_n}{S_m}\left(\frac{1}{\epsilon_m} - 1\right)}$$

$$E_{m,p} \text{ (blades to insert) } = \frac{1}{\frac{1}{\overline{\overline{F}}_{m,p}} + \left(\frac{1}{\epsilon_m} - 1\right) + \frac{S_m}{S_p}\left(\frac{1}{\epsilon_p} - 1\right)}$$

F centrifugal force, lb

$\left\{\begin{matrix}\overline{\overline{F}}_{n,m}, \\ \overline{\overline{F}}_{m,p}\end{matrix}\right.$ functions of geometrical factors of surfaces (reference 13, p. 58)

G mass velocity relative to blades, lb/(sec)(sq ft)

g acceleration of gravity, 32.2 ft/sec^2

H constant in equation (19)

h heat-transfer coefficient, Btu/(hr)(sq ft)(°F)

h_r general radiation coefficient,

$$\left(\frac{0.173\left[\left(\frac{t_h + 460}{100}\right)^4 - \left(\frac{t_c + 460}{100}\right)\right]^4}{t_h - t_c}\right), \text{Btu/(hr)(sq ft)}(^{\circ}\text{F})$$

J mechanical equivalent of heat, 778 ft-lb/Btu

K constant

k thermal conductivity, Btu/(hr)(sq ft)($^{\circ}$F/ft)

L blade length, ft

M blade Mach number, v/a_g

M_a cooling-air Mach number, V_a/a_a

m mass flow per blade, lb/hr

P total pressure, lb/sq ft absolute

p_s static pressure, lb/sq ft absolute

p perimeter, ft

$\overline{p}$ average blade perimeter, ft

Q heat flow, Btu/hr

R gas constant, 53.3 ft-lb/(lb)($^{\circ}$R)

r radius of turbine, ft

S surface area for radiation, sq ft

s blade stress due to centrifugal force, lb/sq in.

T total temperature, $^{\circ}$F

t temperature, $^{\circ}$F

t_s static temperature, $^{\circ}$F

V relative velocity of fluid, ft/sec

v blade tip speed, ft/sec

w maximum blade width, ft

Y $h_i(p_p + p_i)/m_a c_p$

y distance from blade root to any point on blade, ft

Z $h_i p_i/(h_n b + h_o p_o + h_i p_i + h_p p_i)$

α $(h_n b + h_o p_o)/k_m \bar{p} \theta$

β $h_p p_i/k_m \bar{p} \theta$

γ ratio of specific heats

δ $h_i p_i/k_m \bar{p} \theta$

ε emissivity coefficient

ω angular velocity of blades, radians/sec

μ absolute viscosity, lb/hr-ft

θ blade-wall thickness, ft

η factor in equation (22) for effective gas temperature

η_t turbine-shaft efficiency

ρ density, lb/cu ft

λ root of auxiliary equation in solution of differential equation

Subscripts:

a air (with t refers to effective air temperature)

b minimum hot-gas flow passage per blade

c cold surface

e gas (with t refers to effective gas temperature)

g gas

h hot surface

i	inner blade surface
j	nozzle jet
l	cooling-air passage
m	metal
n	nozzle
o	outer blade surface
p	insert surface (except for c_p)
r	blade root (except for h_r)
t	blade tip (except for η_t)
y	any point on blade
1,3	inlet
2,4	outlet

APPENDIX B

DERIVATION OF EQUATION FOR RADIAL TEMPERATURE DISTRIBUTION IN HOLLOW AIR-COOLED BLADE WITH INSERT

A hollow blade with an insert is considered (fig. 16(a)). The temperature gradient through the wall and the changing blade cross-sectional area are neglected. A heat balance for a small portion of the blade height dy results in the following considerations:

Heat entering:

Q_1 = heat entering by conduction = $k_m \bar{p} \theta \frac{d}{dy}\left(t_m + \frac{dt_m}{dy} dy\right)$
(See reference 3.)

Q_3 = heat entering by radiation from the nozzles and by convection = $(h_n b + h_o p_o)(t_e - t_m)\, dy$
(See reference 13.)

Heat leaving:

Q_2 = heat leaving by conduction = $k_m \bar{p} \theta \frac{dt_m}{dy}$

Q_4 = heat leaving by convection and by radiation to the insert = $h_i p_i (t_m - t_a)\, dy + h_p p_i (t_m - t_p)\, dy$

Heat balance:

$$Q_1 + Q_3 - Q_2 - Q_4 = 0$$

or, by substitution,

$$k_m \bar{p} \theta \frac{dt_m}{dy} + k_m \bar{p} \theta \frac{d^2 t_m}{dy^2} dy + (h_n b + h_o p_o)(t_e - t_m)\, dy - k_m \bar{p} \theta \frac{dt_m}{dy}$$

$$- h_i p_i (t_m - t_a)\, dy - h_p p_i (t_m - t_p)\, dy = 0$$

By eliminating dy and collecting terms

$$\frac{d^2t_m}{dy^2} - \left(\frac{h_p p_i}{k_m \bar{p}\theta} + \frac{h_i p_i}{k_m \bar{p}\theta} + \frac{h_n b + h_o p_o}{k_m \bar{p}\theta}\right) t_m + \frac{h_i p_i}{k_m \bar{p}\theta} t_a$$

$$+ \frac{h_p p_i}{k_m \bar{p}\theta} t_p + \left(\frac{h_n b + h_o p_o}{k_m \bar{p}\theta}\right) t_e = 0$$

If

$$\alpha = \frac{h_n b + h_o p_o}{k_m \bar{p}\theta}$$

$$\beta = \frac{h_p p_i}{k_m \bar{p}\theta}$$

$$\delta = \frac{h_i p_i}{k_m \bar{p}\theta}$$

then

$$\frac{d^2t_m}{dy^2} - (\alpha + \beta + \delta)\ t_m + \delta t_a + \beta t_p + \alpha t_e = 0 \tag{6}$$

The total rise in temperature of the cooling air relative to the blade is due to (1) the heat absorbed, and (2) the compression of the air in the blade. The two parts are calculated as follows:

(1) Temperature rise due to heat absorbed from blade

$$m_a c_p dT_a = h_i p_i (t_m - t_a)\ dy + h_i p_p (t_p - t_a)\ dy \tag{7}$$

$$dT_a = \left[\frac{h_i p_i}{m_a c_p} t_m - h_i \frac{(p_i + p_p)}{m_a c_p} t_a + \frac{h_i p_p}{m_a c_p} t_p\right] dy \tag{8}$$

(2) Temperature rise due to compression in the blade

The effective air temperature is considered equal to the total temperature of the cooling-air relative to the blade. The temperature rise due to moving a particle of air radially through a strong centrifugal field can be calculated from Bernoulli's equation in differential form for compressible flow in a centrifugal field.

$$\frac{g\,dp_{s,a}}{\rho} + V_a dV_a - \omega^2 r\, dr = 0 \tag{9}$$

Application of the general gas law $p_{s,a} = R\rho(t_{s,a} + 460)$ to Bernoulli's equation leads to

$$g\,\frac{dp_{s,a}}{p_{s,a}}\,R(t_{s,a} + 460) + V_a dV_a = \omega^2 r\, dr$$

Replacement of the pressure term by a static-temperature term, obtained by logarithmic differentiation of the adiabatic relation (it can be shown from compressible flow theory that K is constant along the passage)

$$460 + t_{s,a} = K p_{s,a}^{\left(\frac{\gamma-1}{1}\right)}$$

gives

$$\frac{gR\gamma}{\gamma - 1}\,dt_{s,a} + V_a dV_a = \omega^2 r\, dr$$

However

$$t_{s,a} = T_a - \frac{V_a^2}{2c_p gJ}$$

and

$$dt_{s,a} = dT_a - \frac{V_a dV_a}{c_p gJ}$$

Therefore,

$$\frac{gR\gamma}{\gamma - 1}\,dT_a - \frac{gR\gamma}{\gamma - 1}\,\frac{V_a dV_a}{c_p gJ} + V_a dV_a = \omega^2 r\, dr$$

Because $R = c_p J\left(\frac{\gamma - 1}{\gamma}\right)$

$$dT_a = \frac{\omega^2 r\, dr}{c_p gJ}$$

But $r = y + r_r$ and $dr = dy$; that is,

$$dT_a = \left(\frac{\omega^2 y}{gc_pJ} + \frac{\omega^2 r_r}{gc_pJ}\right)dy \tag{10}$$

With the assumption that $dT_a = dt_a$, because $\frac{d}{dr}\left[(1-\eta)\ \frac{Va^2}{2gJc_p}\right]$ is small, addition of equations (8) and (10) gives

$$dt_a = \left[\frac{h_ip_i}{m_ac_p}\ t_m + \frac{h_ip_p}{m_ac_p}\ t_p + \frac{\omega^2}{gc_pJ}(y + r_r) - \frac{h_i(p_p + p_i)}{m_ac_p}\ t_a\right]dy \tag{11}$$

The value of t_a obtained by solving equation (6) is

$$t_a = -\frac{1}{\delta}\frac{d^2t_m}{dy^2} + \frac{1}{\delta}\ (\alpha + \beta + \delta)\ t_m - \frac{\beta}{\delta}\ t_p - \frac{\alpha}{\delta}\ t_e \tag{12}$$

Differentiation of equation (12) shows

$$\frac{dt_a}{dy} = -\frac{1}{\delta}\frac{d^3t_m}{dy^3} + \frac{1}{\delta}\ (\alpha + \beta + \delta)\ \frac{dt_m}{dy} \tag{13}$$

Equating equations (11) and (13), using equation (12) for t_a, and letting

$$\frac{h_i(p_p + p_i)}{m_ac_p} = Y$$

results in

$$-\frac{1}{\delta}\frac{d^3t_m}{dy^3} - \frac{Y}{\delta}\frac{d^2t_m}{dy^2} + \frac{1}{\delta}\ (\alpha + \beta + \delta)\ \frac{dt_m}{dy} + \left[\frac{Y}{\delta}\ (\alpha + \beta + \delta) - \frac{h_ip_i}{m_ac_p}\right]t_m$$

$$= \frac{\omega^2}{gc_pJ}\ y + \left[\frac{\omega^2 r_r}{gc_pJ} + \frac{h_ip_p}{m_ac_p}\ t_p + \frac{Y}{\delta}\ (\beta t_p + \alpha t_e)\right]$$

The result of changing sign and multiplying by δ is

$$\frac{d^3t_m}{dy^3} + Y\frac{d^2t_m}{dy^2} - (\alpha + \beta + \delta)\frac{dt_m}{dy} + \left[\frac{h_i p_i}{m_a c_p}\delta - Y(\alpha + \beta + \delta)\right]t_m$$

$$= -\frac{\omega^2\delta}{gc_pJ}y - \left[\frac{\omega^2\delta}{gc_pJ}r_r + \left(\frac{h_i p_p}{m_a c_p}\delta + Y\beta\right)t_p + Y\alpha t_e\right] \tag{1}$$

which can be rewritten as

$$(D^3 + a_1D^2 + a_2D + a_3)\ t_m = a_4y + a_5 \tag{14}$$

where a_1, a_2, a_3, a_4, and a_5 are the coefficients of equation (1) and are constants for a chosen set of turbine operating conditions. A solution of this equation is

$$t_m = c_1e^{\lambda_1 y} + c_2e^{\lambda_2 y} + c_3e^{\lambda_3 y} + c_4y + c_5 \tag{2}$$

The constants λ_1, λ_2, and λ_3 are the roots of the cubic equation (in the parentheses) of the left member of equation (14) set equal to zero. This cubic equation was solved numerically by Horner's method.

The constants c_1, c_2, and c_3 are determined from the following boundary conditions:

$t_{m,r}$ = a constant, when $y = 0$.

$t_{a,r}$ = a constant, when $y = 0$.

$dt_m/dy = 0$, when $y = L$. (15)

The constants c_4 and c_5 are found as follows:

(a) Divide unity by $a_3 + a_2D + a_1D^2 + D^3$ (the term in the parenthesis in the left member of equation (14)).

(b) The result is of the form $A_1 + A_2D + \ldots$, where D denotes differentiation. Because the right member of equation (14) is linear, the division may be stopped after the second term $(A_1 + A_2D)$ inasmuch as all derivatives of orders higher than the first vanish.

(c) This result is then used as an operator on the right member of equation (14), or $(A_1 + A_2D)(a_4y + a_5)$, which results in $A_1a_4y + A_1a_5 + A_2a_4$.

(d) c_4 is then $A_1a_5 + A_2a_4$.

(e) c_5 is A_1a_4.

The relation between the air and metal temperatures, given by equation (12), is rewritten as

$$t_a = K_1 \frac{d^2t_m}{dy^2} + K_2t_m + K_3t_p + K_4t_e \tag{16}$$

where K_1, K_2, K_3, K_4, t_p, and t_e are all known constants. Differentiation of equation (14) gives

$$\frac{dt_m}{dy} = c_1\lambda_1e^{\lambda_1y} + c_2\lambda_2e^{\lambda_2y} + c_3\lambda_3e^{\lambda_3y} + c_4 \tag{17}$$

Differentiation of equation (17) gives

$$\frac{d^2t_m}{dy^2} = c_1\lambda_1{}^2e^{\lambda_1y} + c_2\lambda_2{}^2e^{\lambda_2y} + c_3\lambda_3{}^2e^{\lambda_3y} \tag{18}$$

From equations (2) and (15) for $y = 0$,

$$c_1 + c_2 + c_3 + c_5 = \text{constant} = H \tag{19}$$

From equations (17) and (15) for $y = L$,

$$c_1\lambda_1e^{L\lambda_1} + c_2\lambda_2e^{L\lambda_2} + c_3\lambda_3e^{L\lambda_3} + c_4 = 0 \tag{20}$$

From equations (16), (18), (2), and (15) for $y = 0$,

$$K_1\left(c_1\lambda_1{}^2 + c_2\lambda_2{}^2 + c_3\lambda_3{}^2\right) + K_2H + K_3t_p + K_4t_e = t_{a,r} = \text{constant} \tag{21}$$

Simultaneous solution of equations (19), (20), and (21) results in the desired values of the constants c_1, c_2, and c_3.

APPENDIX C

DERIVATION OF EQUATION FOR RADIAL STRESS DISTRIBUTION IN LINEARLY TAPERED TURBINE BLADE

The hollow turbine blade (fig. 16(b)) has a length L, a cross-sectional area $A_{m,t}$ at the tip and $A_{m,r}$ at the root. The centrifugal force on any section dy is

$$dF = \frac{\rho_m \omega^2}{g} r_y A_{m,y} dy$$

The total force on cross section $A_{m,y}$ is

$$F = \int_y^L \frac{\rho_m \omega^2}{g} r_y A_y dy$$

For a linear variation in cross-sectional area from root to tip

$$A_y = \frac{(A_{m,t} - A_{m,r})}{L} y + A_{m,r}$$

and

$$r_y = r_t - (L - y)$$

$$F = \frac{\rho_m \omega^2}{g} \left[\int_y^L (r_t y - Ly + y^2) \frac{(A_{m,t} - A_{m,r})}{L} dy + \int_y^L A_{m,r} (r_t - L + y) dy \right]$$

After integration,

$$F = \frac{\rho_m \omega^2}{g} \left[\frac{(A_{m,t} - A_{m,r})}{L} \left(\frac{r_t y^2}{2} - \frac{Ly^2}{2} + \frac{y^3}{3} \right) + A_{m,r} \left(r_t y - Ly + \frac{y^2}{2} \right) \right]_y^L$$

The stress is

$$\frac{F}{A} = \frac{\rho_m \omega^2}{g} \frac{A_{m,r}}{(A_{m,t} - A_{m,r}) \frac{y}{L} + A_{m,r}}$$

$$\left\{\left(\frac{A_{m,t}}{A_{m,r}} - 1\right)\left[\left(\frac{r_t}{L} - 1\right)\frac{y^2}{2} + \frac{y}{L}\frac{y^2}{3}\right] + (r_t - L)\ y + \frac{y^2}{2}\right]_y^L\right\}$$

and

$$s = \frac{\rho_m v^2}{2g\left[\left(\frac{A_{m,t}}{A_{m,r}} - 1\right)\frac{y}{L} + 1\right]}\left\{\left(\frac{A_{m,t}}{A_{m,r}} - 1\right)\left[\frac{r_t}{L} - 1 + \frac{2}{3}\frac{y}{L}\right]\left(\frac{y}{r_t}\right)^2\right.$$

$$\left. + \left[2\left(1 - \frac{L}{r_t}\right)\frac{y}{r_t} + \left(\frac{y}{r_t}\right)^2\right]_y^L\right\} \qquad (3)$$

In this form, for a given blade metal, given ratios of $A_{m,t}/A_{m,r}$ and L/r_t, and a given blade length the stress is a function only of tip speed v.

APPENDIX D

CALCULATION OF RATIO OF EFFECTIVE GAS TEMPERATURE TO TURBINE-INLET TEMPERATURE

The effective gas temperature for heat transmission is determined by the relation

$$t_e = t_{s,g} + \eta \frac{V_g^{\,2}}{2gJc_p}$$

where $\eta = 0.85$ (reference 10, p. 10). In reference 7, the value $\eta = 1$ was used.

The turbine-inlet total temperature is

$$T_g = t_{s,g} + \frac{V_j^{\,2}}{2gJc_p}$$

Because of the assumptions of shock-free entry and of constant cross-sectional area, the two values of $t_{s,g}$ are the same. Hence, by eliminating $t_{s,g}$ between the two equations,

$$t_e = T_g - \frac{V_j^{\,2}}{2gc_pJ} + \frac{0.85\ V_g^{\,2}}{2gc_pJ} = T_g - \frac{V_j^{\,2}}{2gc_pJ}\left[1 - 0.85\left(\frac{V_g}{V_j}\right)^2\right]$$

For a typical ideal impulse turbine with a 25° nozzle angle at peak efficiency, $v_t/V_j = 0.5$ and $V_g/V_j = 0.6$, $V_g = V_j - V_t$; or $V_g/V_j = 1 - V_t/V_j = 0.5$. Changing to absolute temperatures

$$(t_e + 460) = (T_g + 460) - \frac{V_j^{\,2}}{2gc_pJ}\left[1 - 0.85\ (0.6)^2\right]$$

$$= (T_g + 460) - 0.694\ \frac{V_j^{\,2}}{2gc_pJ}$$

If the gas at the nozzle exit flows with the speed of sound, the velocity of the gas based on the inlet total temperature becomes

$$V_j^{\,2} = \frac{2\gamma}{\gamma + 1} gR\ (T_g + 460)$$

Then

$$(t_e + 460) = (T_g + 460) - 0.694 \left(\frac{\gamma - 1}{\gamma + 1}\right)(T_g + 460)$$

and assuming $\gamma = 1.31$ corresponding to temperatures in the range of 2000° F,

$$\frac{(t_e + 460)}{(T_g + 460)} = (1 - 0.093) = 0.907 \qquad (23)$$

REFERENCES

1. Reuter, J. George, and Gazley, Carl, Jr.: Computed Temperature Distribution and Cooling of Solid Gas-Turbine Blades. NACA RM No. E7B11h, 1947.

2. Brown, W. Byron: Cooling of Gas Turbines. I - Effects of Addition of Fins to Blade Tips and Rotor, Admission of Cooling Air through Part of Nozzles, and Change in Thermal Conductivity of Turbine Components. NACA RM No. E7B11a, 1947.

3. Wolfenstein, Lincoln, Meyer, Gene L., and McCarthy, John S.: Cooling of Gas Turbines. II - Effectiveness of Rim Cooling of Blades. NACA RM No. E7B11b, 1947.

4. Sanders, J. C., and Mendelson, Alexander: Theoretical Evaluation of Methods of Cooling the Blades of Gas Turbines. NACA RM No. E7B11g, 1947.

5. Brown, W. Byron, and Livingood, John N. B.: Cooling of Gas Turbines. III - Analysis of Rotor and Blade Temperatures in Liquid-Cooled Gas Turbines. NACA RM No. E7B11c, 1947.

6. Brown, W. Byron, and Monroe, William R.: Cooling of Gas Turbines. IV - Calculated Temperature Distribution in the Trailing Part of a Turbine Blade Using Direct Liquid Cooling. NACA RM No. E7B11d, 1947.

7. Wolfenstein, Lincoln, Maxwell, Robert L., and McCarthy, John S.: Cooling of Gas Turbines. V - Effectiveness of Air Cooling of Hollow Blades. NACA RM No. E7B11e, 1947.

8. Livingood, John N. B., and Sams, Eldon W.: Cooling of Gas Turbines. VI - Computed Temperature Distribution Through Cross Section of Water-Cooled Turbine Blade. NACA RM No. E7B11f, 1947.

9. Müller, K. J.: Theoretical Investigations on Cooling of Gas Turbines. Navy Dept. Trans. No. 198, David Taylor Model Basin, Washington, D. C., March 1946. (From Deutsche Luftfahrtforschung Forschungsbericht No. 1918.)

10. Pollman, Erich: Temperaturen und Beanspruchungen an Hohlschaufeln für Gasturbinen. Deutsche Luftfahrtforschung, Forschungsbericht Nr. 1879, ZWB, July 30, 1943.

11. Kuppers, K. H.: Temperaturenmessungen an zwei ruhenden Gasturbinen-Schaufelprofilen mit Grenzschichtkühlung, DVL, UM, Nr. 1171, ZWB, Feb. 2, 1944.

12. Kress, H.: Verminderung der Leistungsverluste innengekühlter Turbinen. DVL E. V., Inst. f. motorische Arbeitsverfahren u. Thermodynamik, Berlin-Adlershof, Forschungsbericht Nr. 1887, ZWB, Dec. 10, 1943.

13. McAdams, William H.: Heat Transmission. McGraw-Hill Book Co., Inc., 2d ed., 1942.

14. Machlin, E. S., and Nowick, A. S.: Stress Rupture of Heat-Resisting Alloys as a Rate Process. NACA TN No. 1126, 1946.

TABLE I - TURBINE-BLADE DIMENSIONS

Blade	Number of blades B	Blade length L (ft)	Tip radius r_t (ft)	Wall thickness at tip θ_t (in.)	Wall thickness at root θ_r (in.)	Perimeter of outside blade wall p_o (ft)	Perimeter of inside blade wall p_i (ft)	Perimeter of insert p_p (ft)	Area of external cross section A_o (sq ft)	Area of cooling-air passage A_l (sq ft)	Minimum hot-gas-flow area per blade A_b (sq ft)	Ratio of cooling-air area to minimum hot-gas-flow area A_l/A_b	Maximum blade width w (ft)
1								0		0.00241		0.990	
2	54	0.333	1.083	0.020	0.060	0.385	0.314	.325	0.00424	.00169	0.02435	.694	0.0333
3								.3125		.00109		.447	

TABLE II - TURBINE OPERATING CONDITIONS

Hot-gas mass flow per blade, m_g, lb/hr	5260
Cooling-air mass flow per blade, m_a, lb/hr	Dilution × 5260
Total pressure at turbine-nozzle inlet, $P_{n,1}$, lb/sq ft	8480
Mass velocity of hot gas, G_g, lb/(sec)(sq ft)	216,000
Hot-gas heat-transfer coefficient, h_o, Btu/(hr)(sq ft)(°F)	198
Cooling-air temperature at root, $t_{a,r}$, °F	400
Effective hot-gas temperature (also nozzle temperature), t_e, °F	1700, 1900
Average insert temperature, t_p, °F	
Blade 2	600
Blade 3	700
Cooling-air Mach number, M_a	Less than 0.50
Radiation coefficient from nozzle to blade wall for temperature of 1700° F, h_n, Btu/(hr)(sq ft)(°F)	43
Radiation coefficient from nozzle to blade wall for temperature of 1900° F, h_n, Btu/(hr)(sq ft)(°F)	56
Radiation coefficient from blade wall to insert surface, h_p, Btu/(hr)(sq ft)(°F)	12
Nozzle-surface emissivity for temperatures of 1700° and 1900° F, ϵ_n	0.95
Insert-surface emissivity for temperatures of 600° and 700° F, ϵ_p	0.50
Blade-wall emissivity at average temperature of 1400° F, ϵ_m	0.90
Design rotational speed, rpm	11,500
Design blade tip speed, v, ft/sec	1300

National Advisory Committee
for Aeronautics

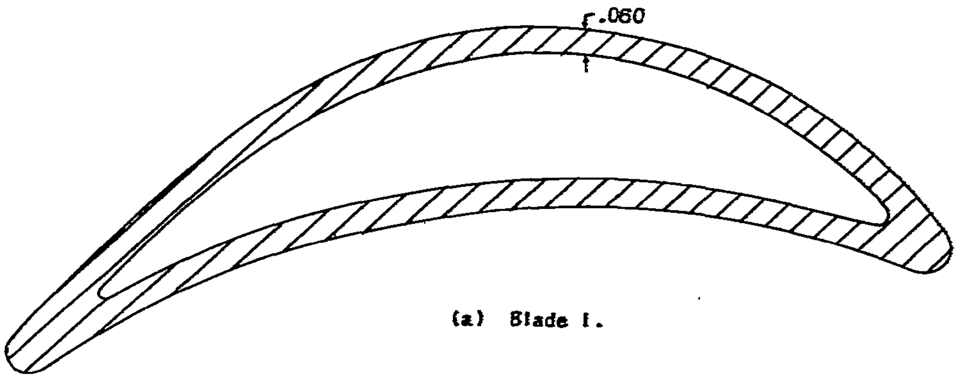

(a) Blade 1.

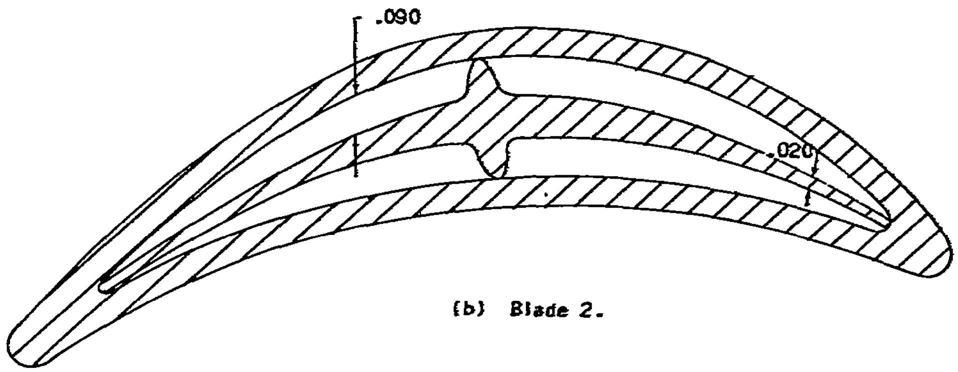

(b) Blade 2.

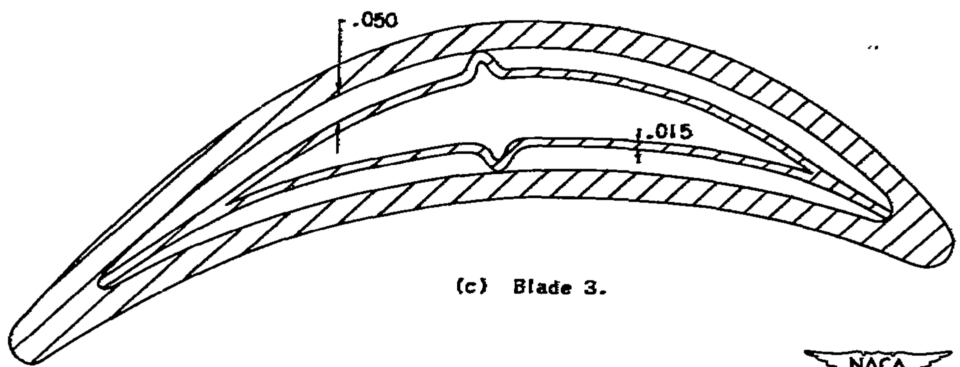

(c) Blade 3.

Figure 1. - Sketches of root section of air-cooled turbine blades. (All dimensions in inches.)

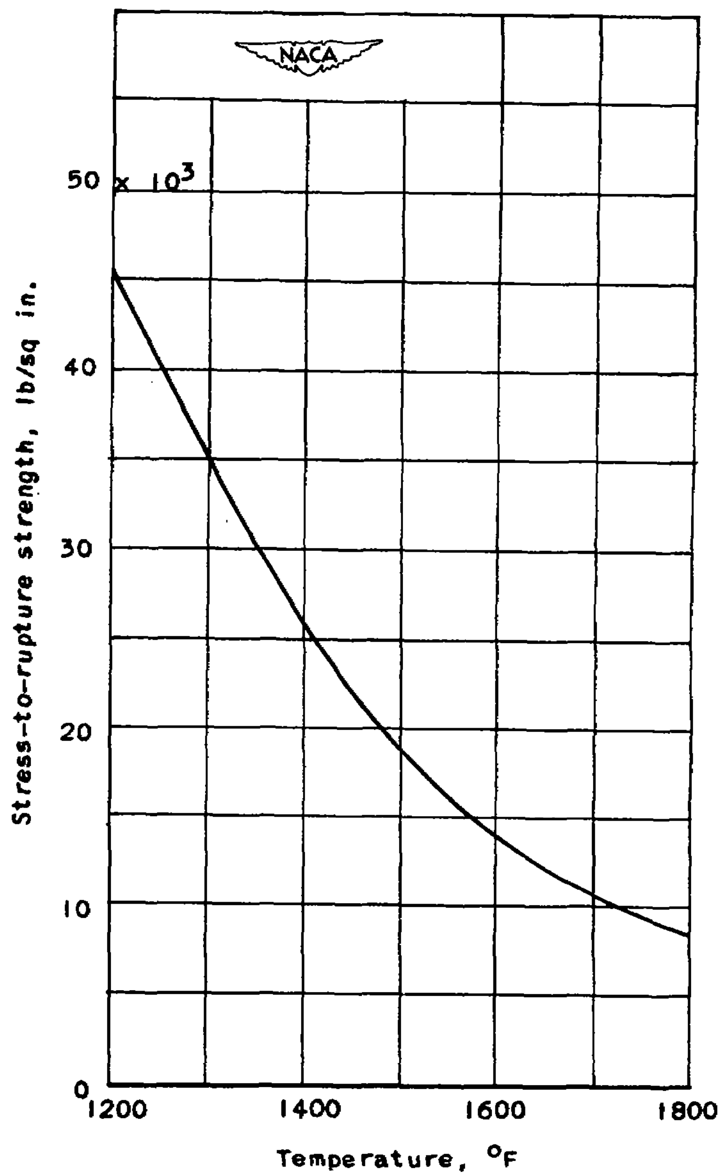

Figure 2. - Stress-to-rupture strength for 1000-hour life for cast S-816.

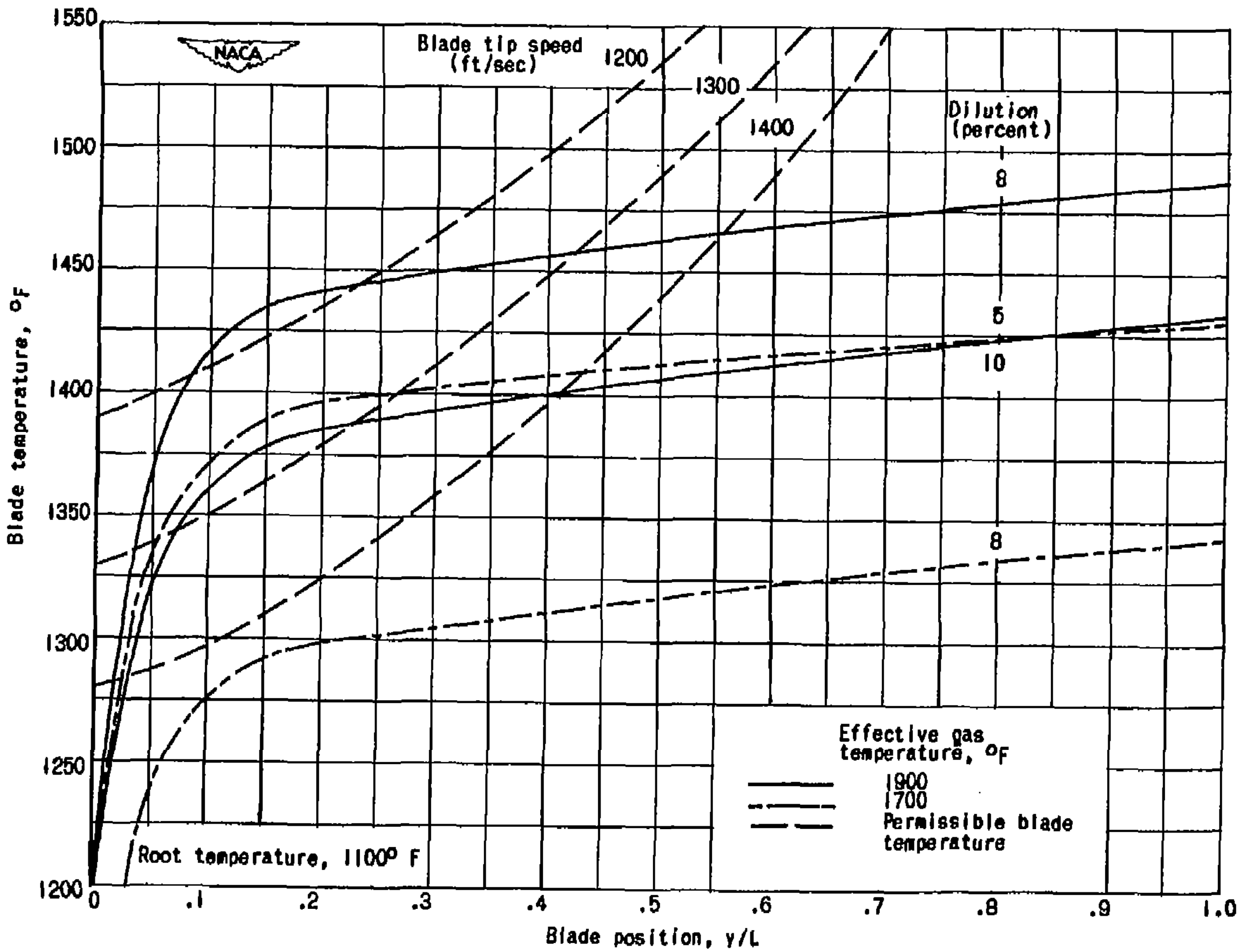

Figure 3. - Temperature distributions for various dilutions in blade I. Blade-root cooling-air temperature, 400° F.

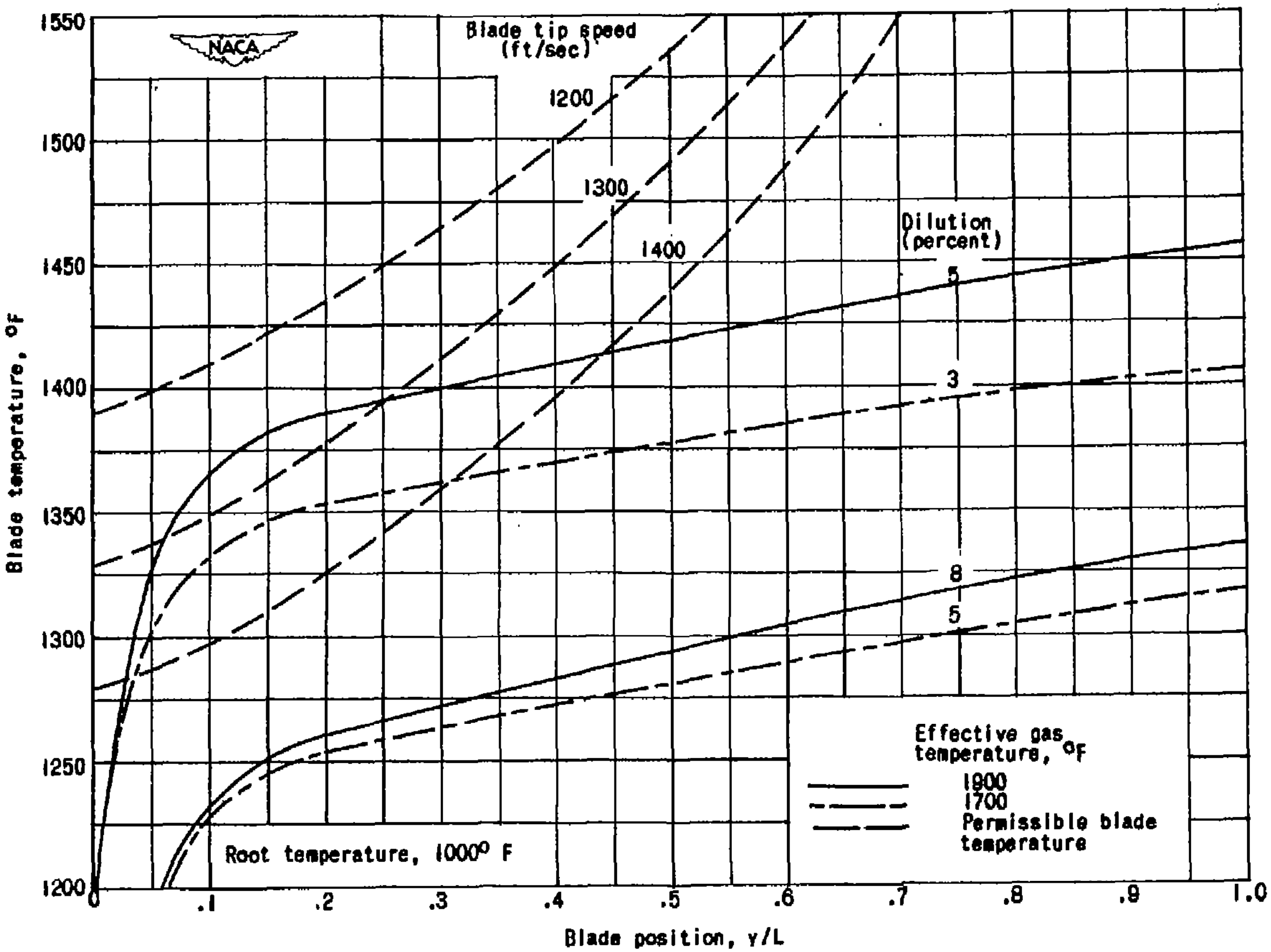

Figure 4. - Temperature distributions for various dilutions in blade 2. Blade-root cooling-air temperature, 400° F; average insert temperature, 600° F.

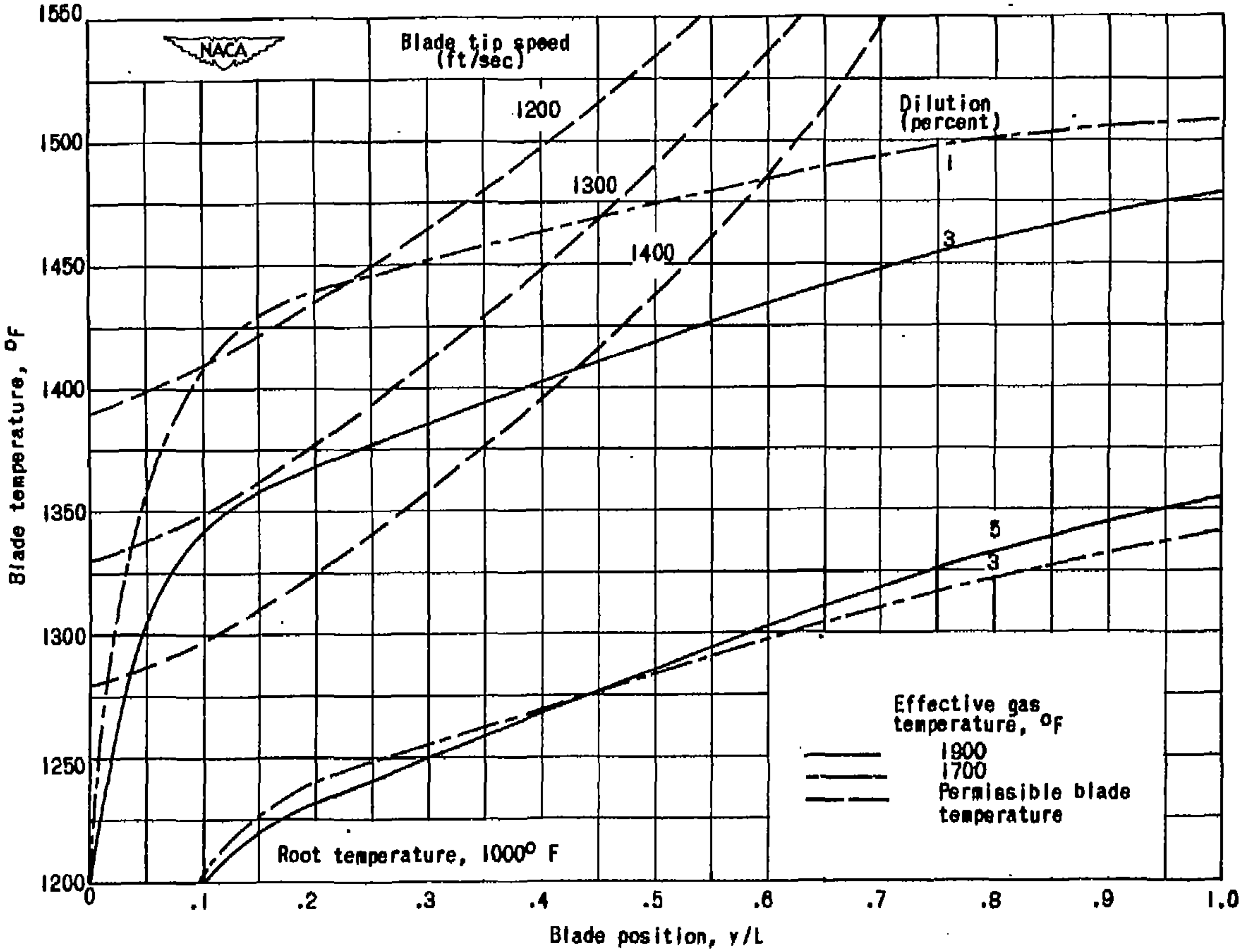

Figure 5. - Temperature distributions for various dilutions in blade 3. Blade-root cooling-air temperature, 400° F; average insert temperature, 700° F.

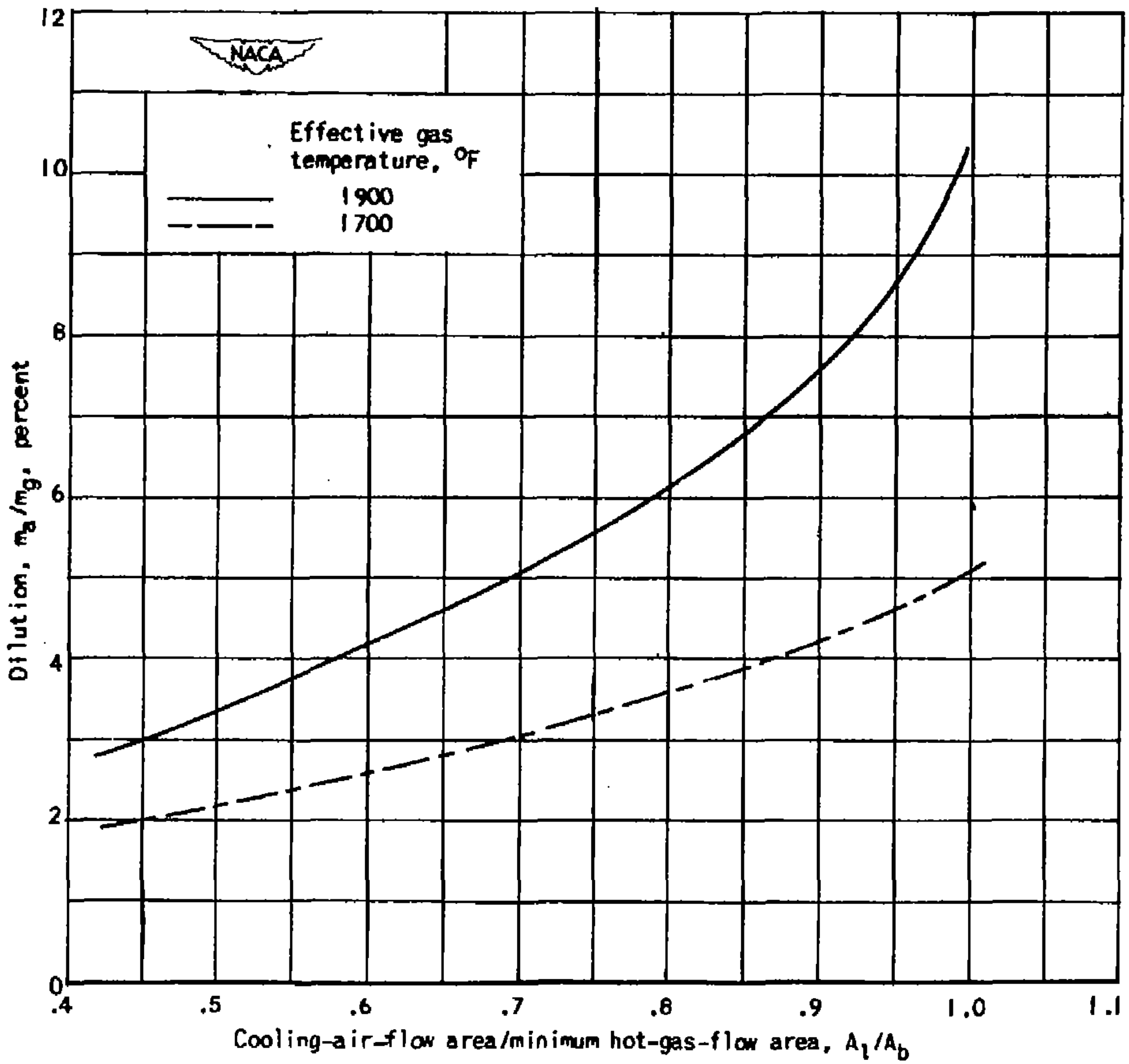

Figure 6. - Effect of flow-area ratio on dilution.

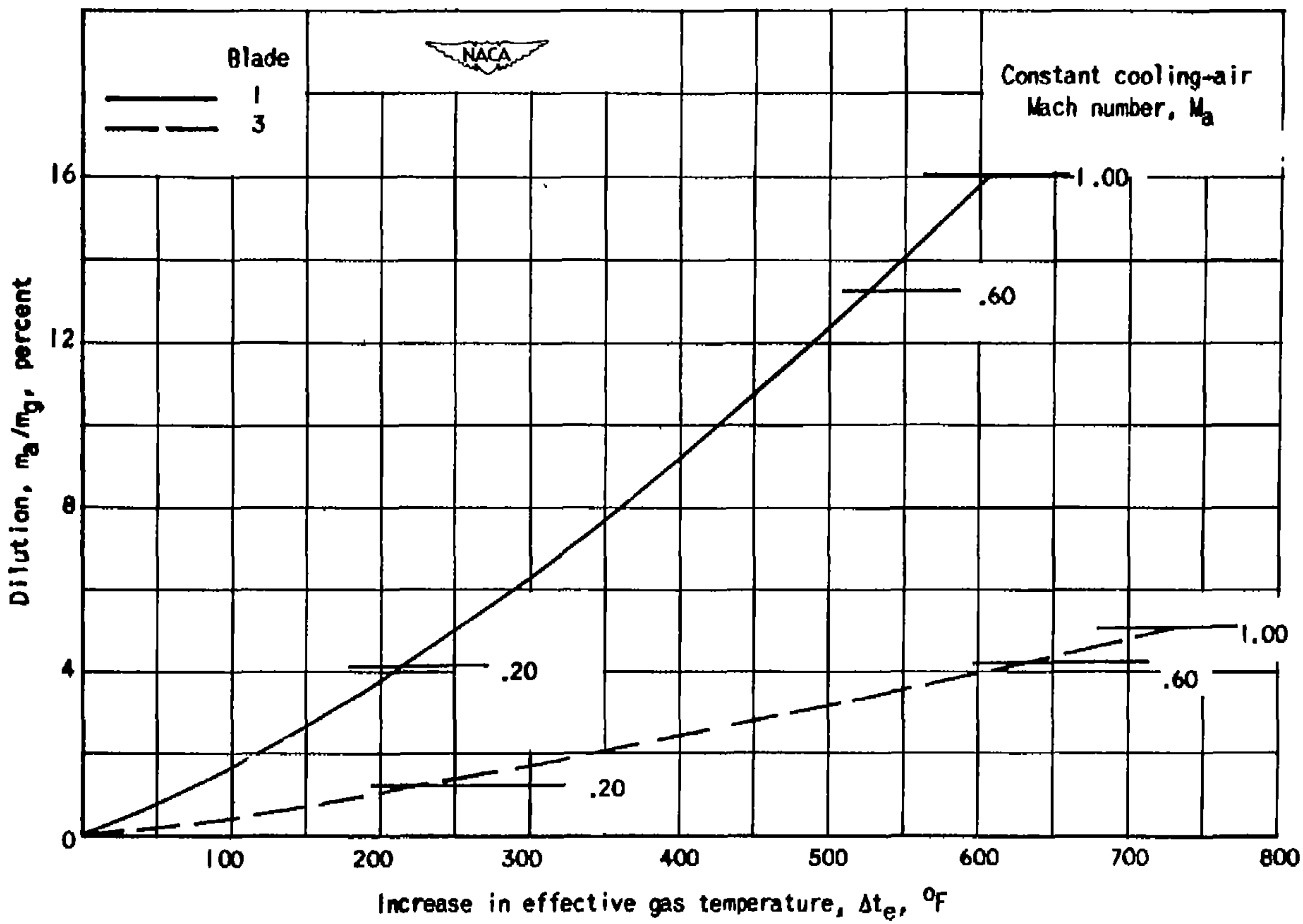

Figure 7. - Air cooling of hollow turbine blade for life of 1000 hours and blade Mach number of 0.50.

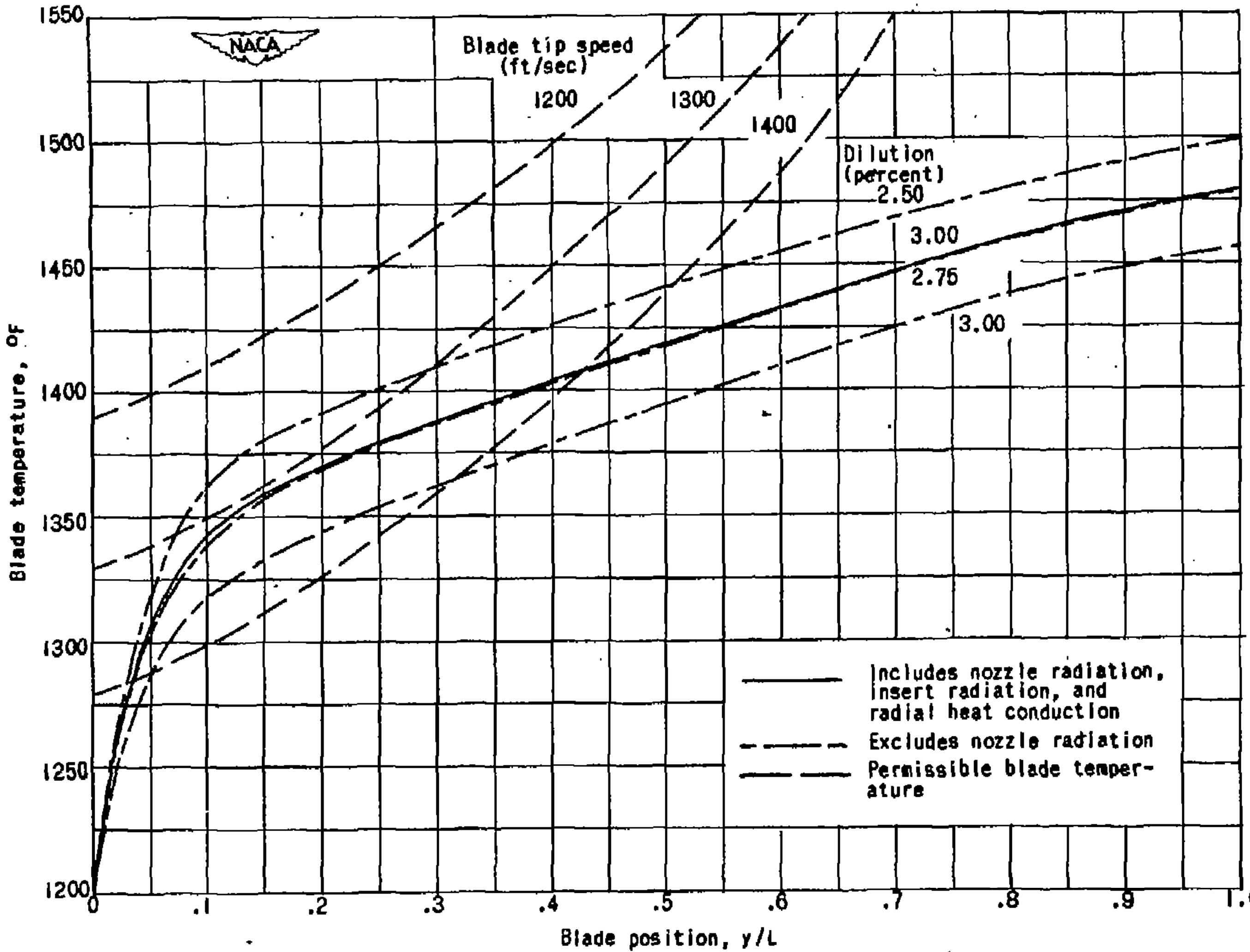

Figure 8. - Effect on dilution of neglecting radiation from nozzles to turbine-blade wall in blade 3. Effective gas temperature, 1900° F; average insert temperature, 700° F; blade-root cooling-air temperature, 400° F.

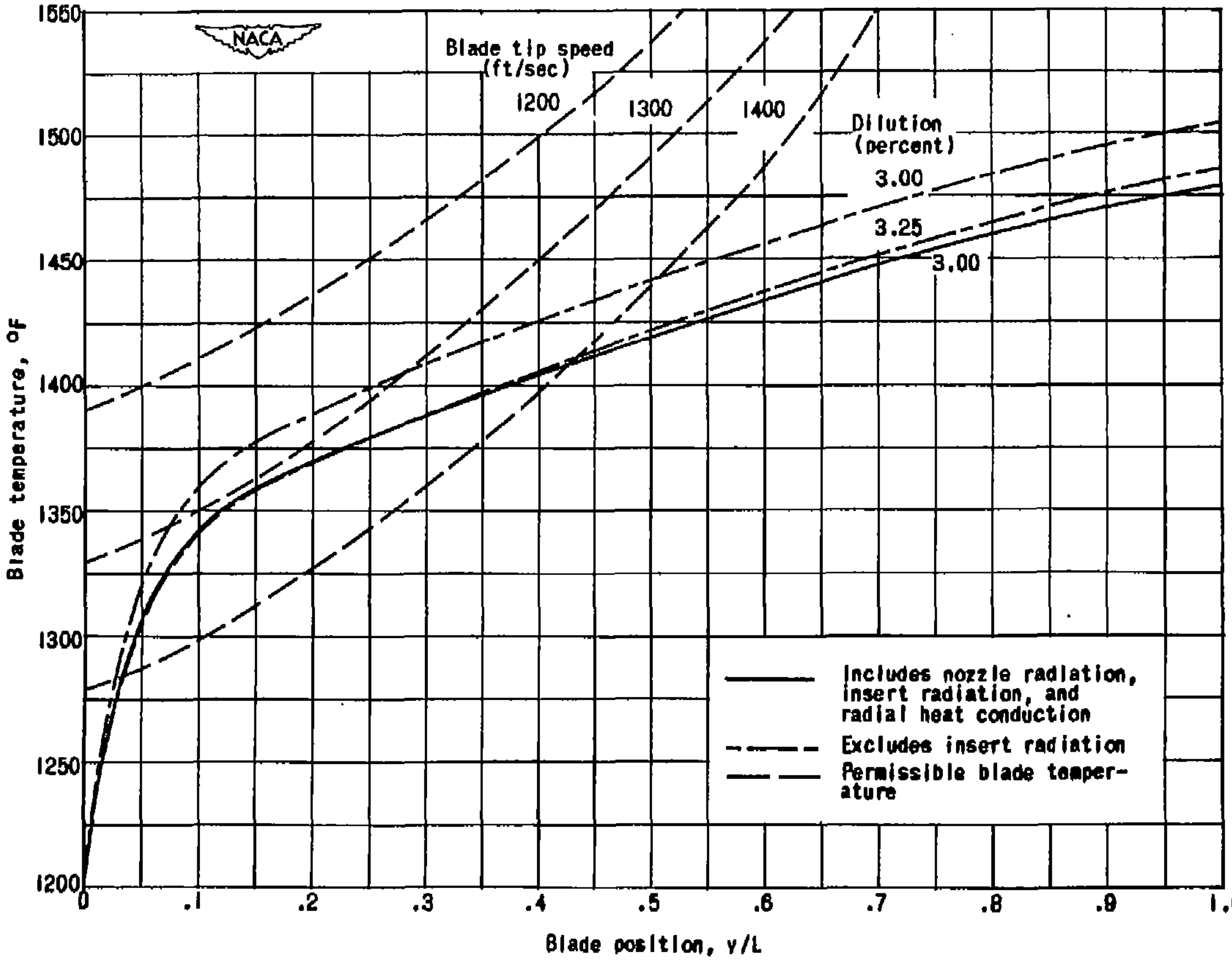

Figure 9. - Effect on dilution of neglecting radiation from inner blade wall to insert in blade 3. Effective gas temperature, 1900° F; average insert temperature, 700° F; blade-root cooling-air temperature, 400° F.

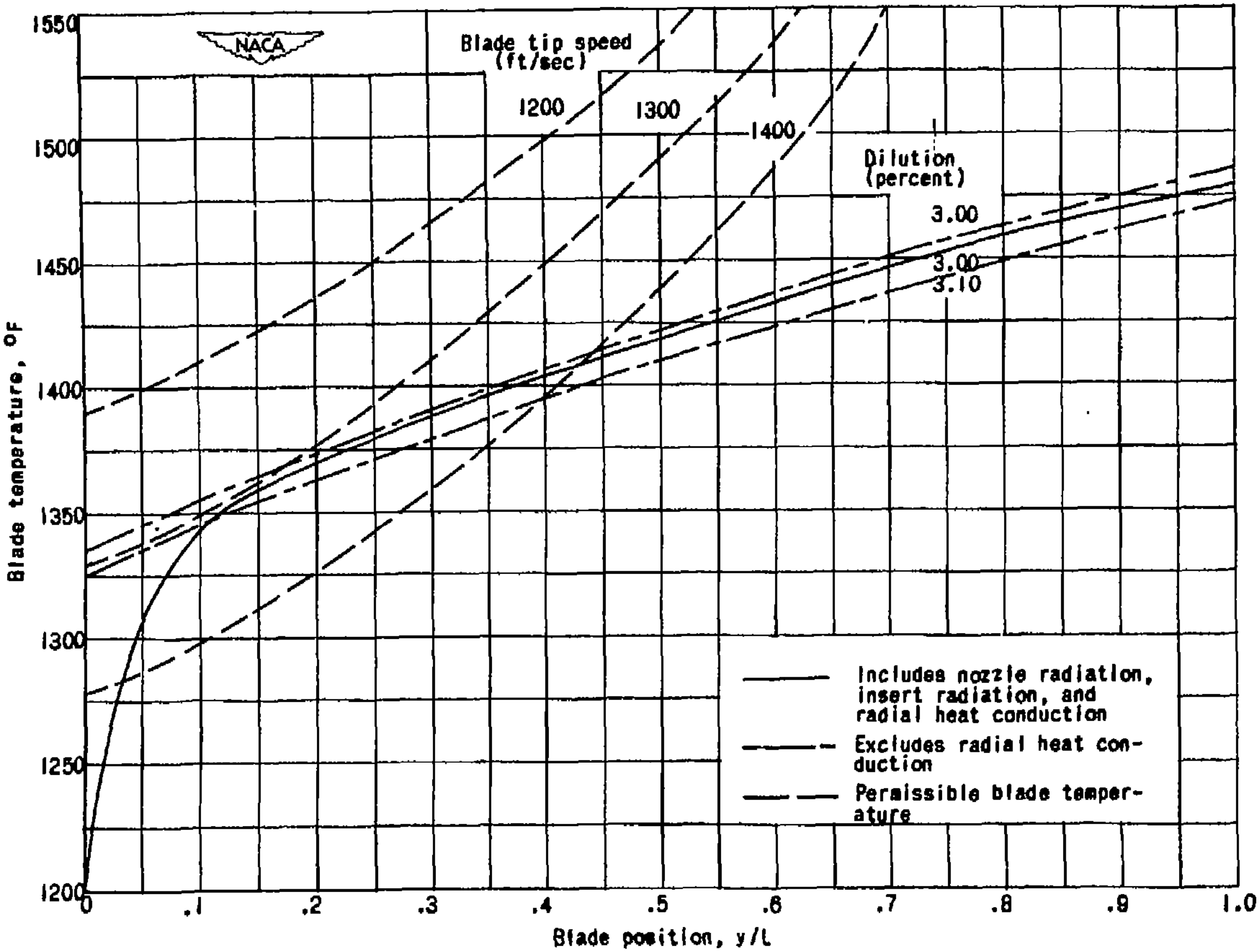

Figure 10. - Effect on dilution of neglecting radial heat conduction in blade 3. Effective gas temperature, 1900° F; average insert temperature, 700° F; blade-root cooling-air temperature, 400° F.

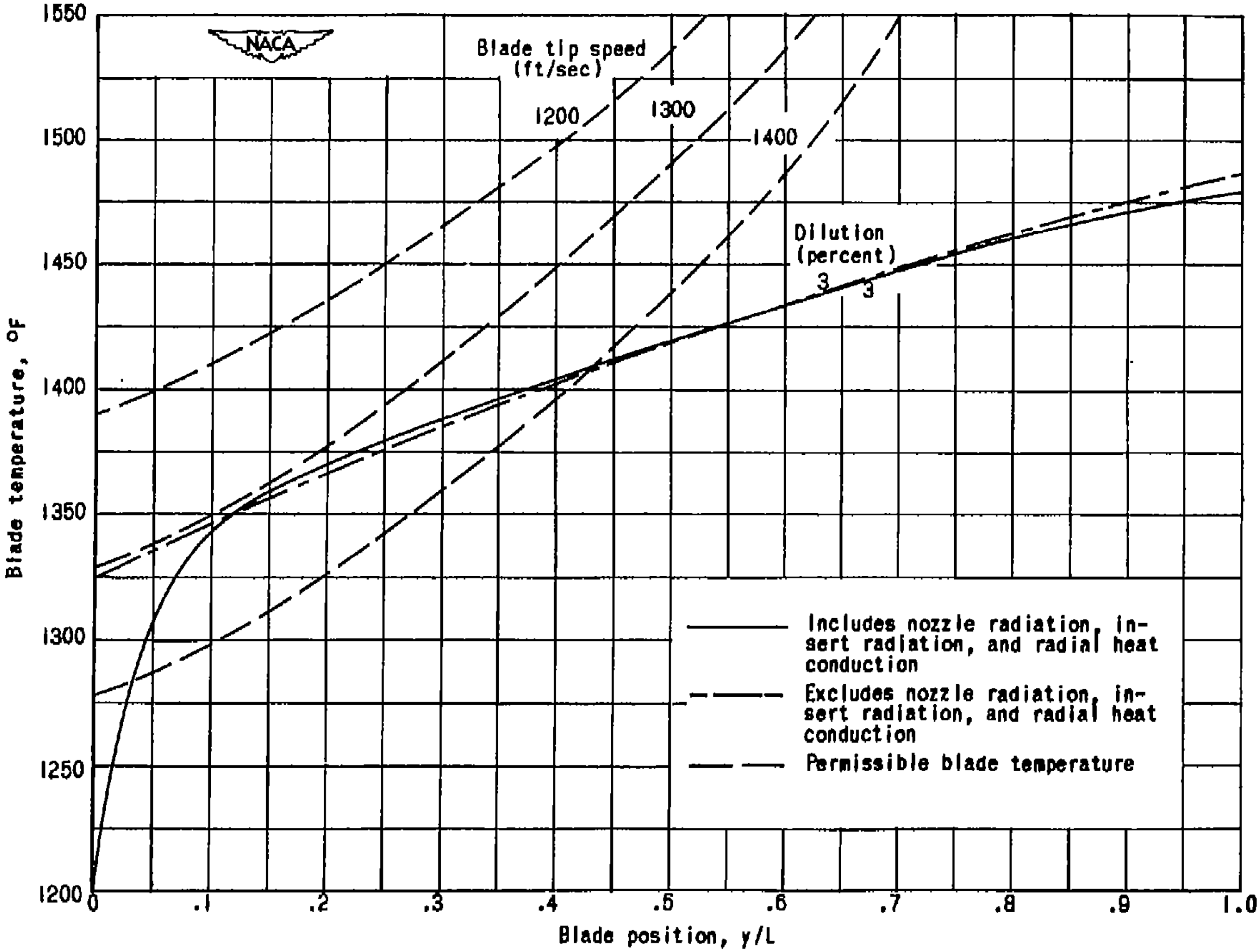

Figure 11. - Effect on dilution of neglecting radiation from nozzles to turbine-blade wall, radiation from inner blade wall to insert, and radial heat conduction in blade 3. Effective gas temperature, 1900° F; average insert temperature, 700° F; blade-root cooling-air temperature, 400° F.

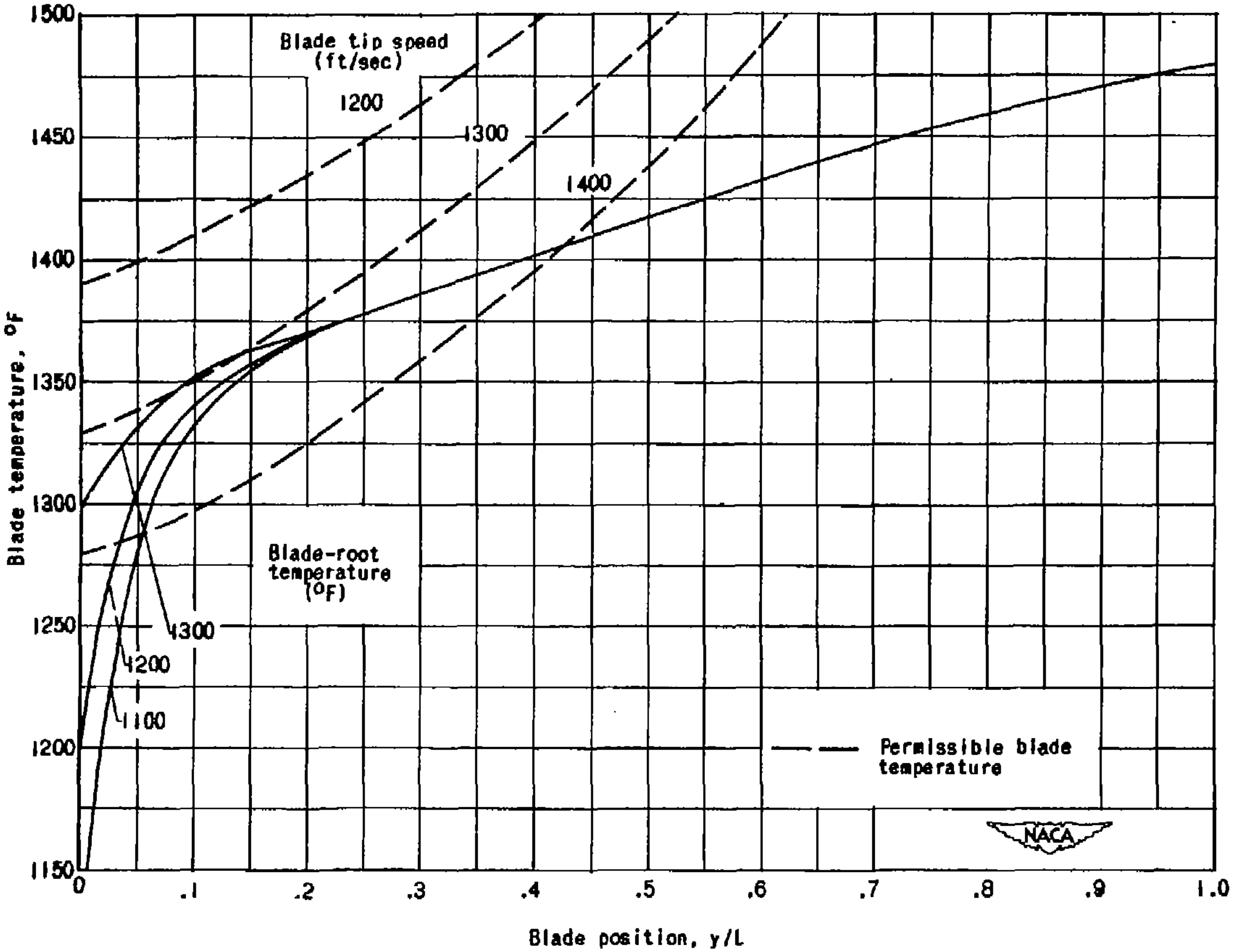

Figure 12. - Effect of blade-root temperature on blade-temperature distribution in blade 3. Dilution, 3 percent; effective gas temperature, 1900° F; average insert temperature, 700° F; blade-root cooling-air temperature, 400° F.

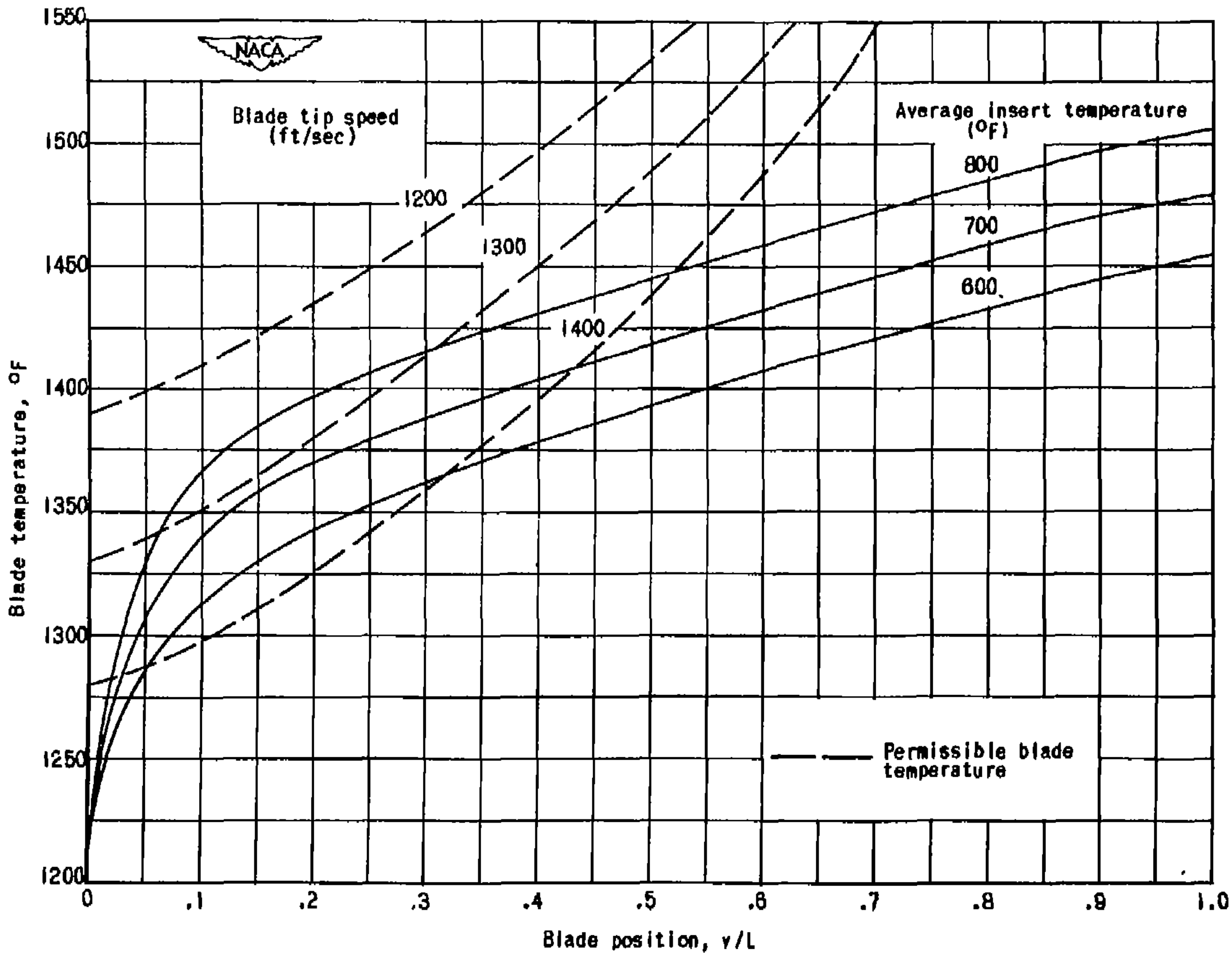

Figure 13. - Effect of average insert temperature on blade-temperature distribution in blade 3. Dilution, 3 percent; effective gas temperature, 1900° F; blade-root cooling-air temperature, 400° F, blade-root temperature, 1200° F.

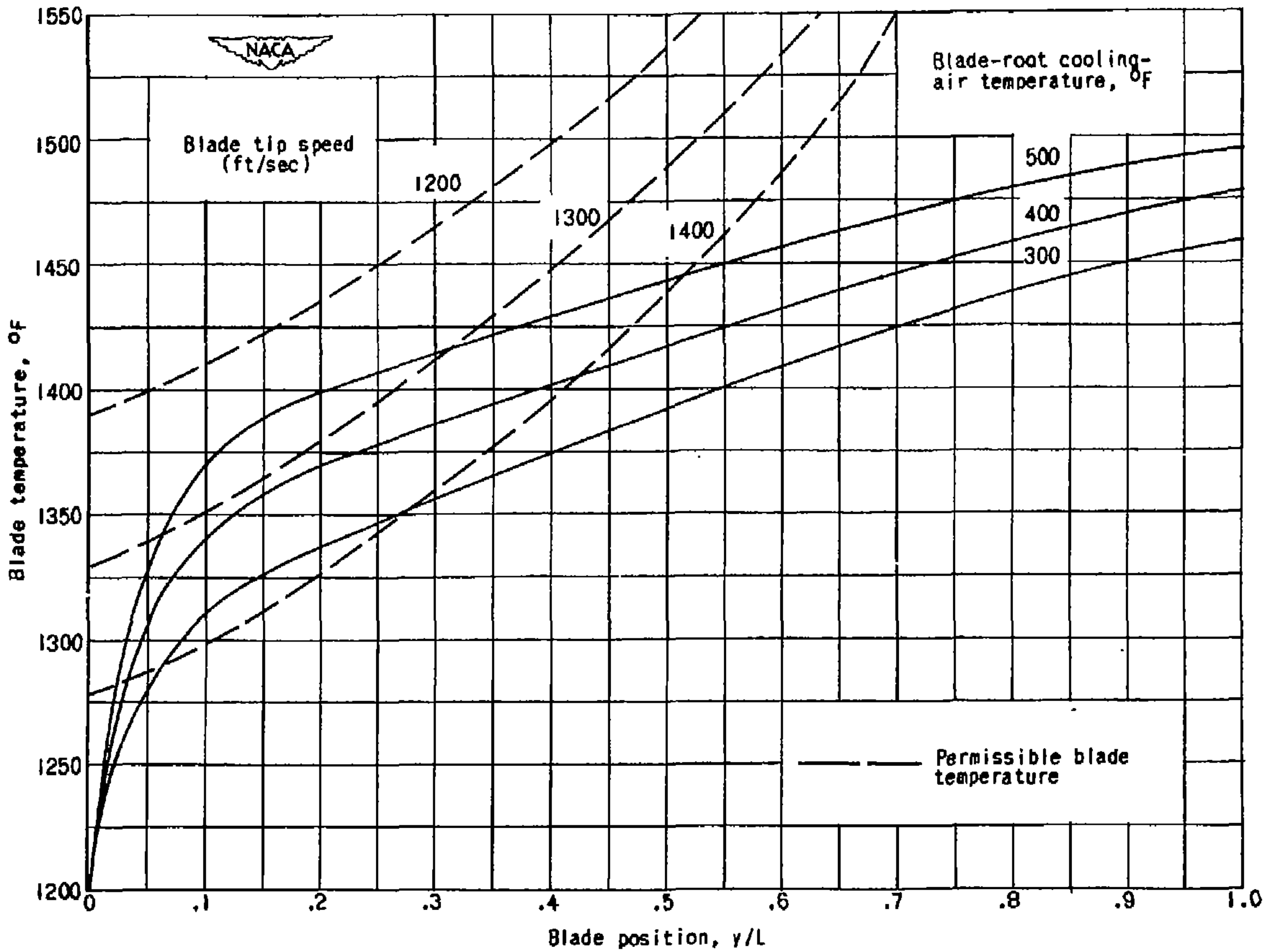

Figure 14. - Effect of blade-root cooling-air temperature on blade-temperature distribution in blade 3. Dilution, ɔ percent; effective gas temperature, 1900° F; average insert temperature, 700° F; blade-root temperature, 1200° F.

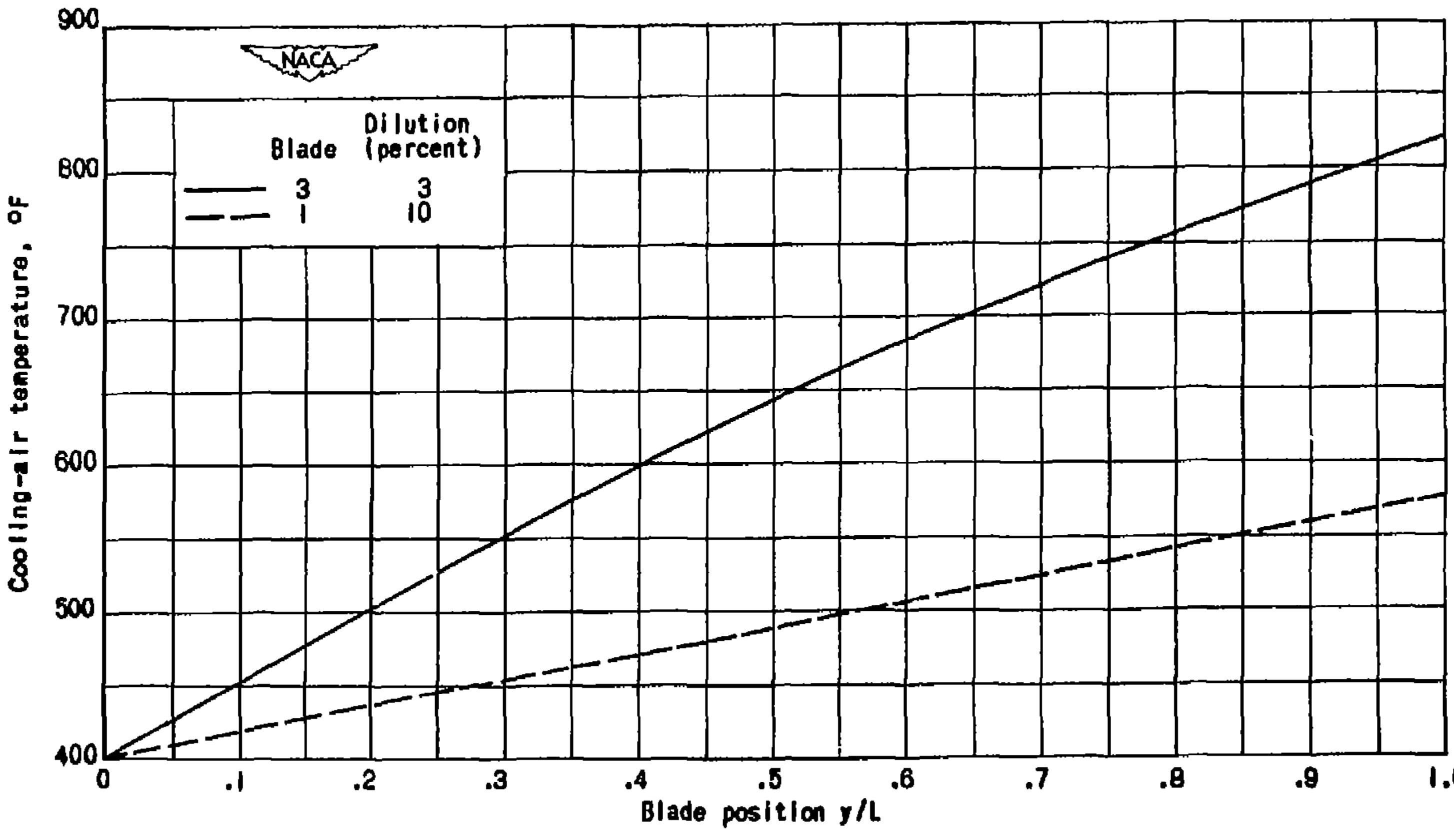

Figure 15. - Cooling-air temperature distribution for blades 1 and 3. Effective gas temperature, 1900° F.

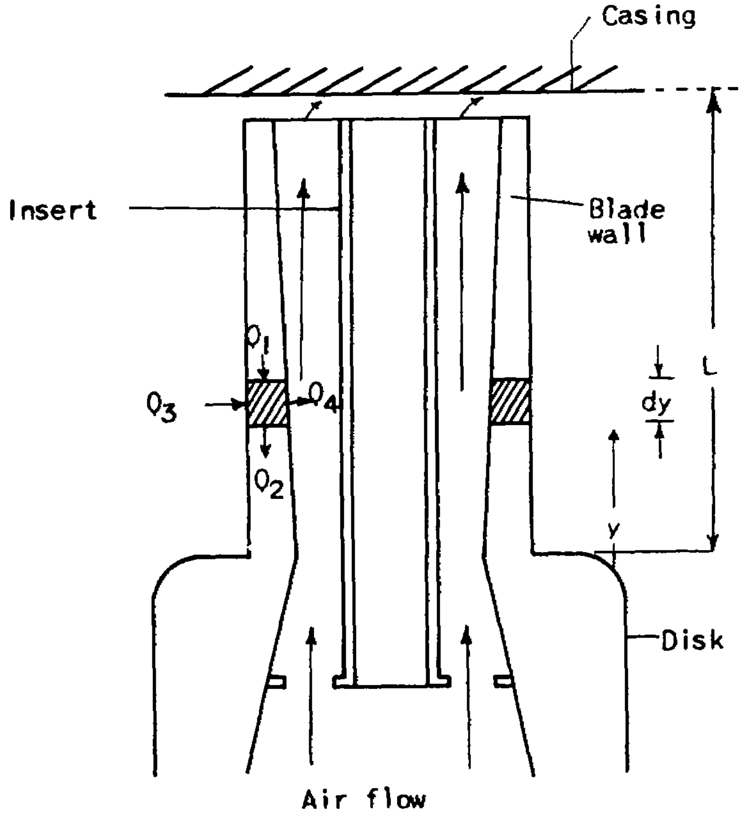

(a) Heat flow in hollow turbine blade with insert.

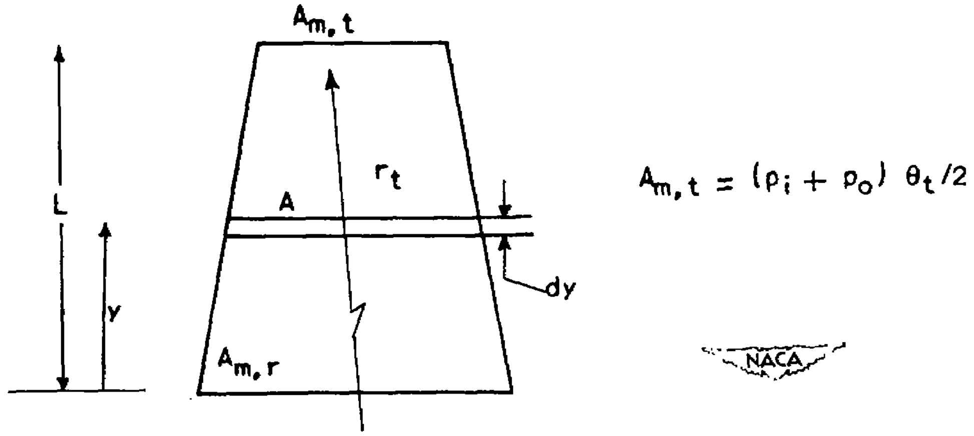

(b) Linearly tapered blade.

Figure 16. - Sketches of turbine blade for temperature and stress analysis.